WRDC-TR-89-4113

COMPUTER TOMOGRAPHY OF THERMAL BATTERIES AND OTHER CLOSED SYSTEMS

Richard H. Bossi

Boeing Aerospace Company
P. O. Box 3999
Seattle WA 98124

December 1989

Interim Report For Period August 1988 - June 1989

MATERIALS LABORATORY
WRIGHT RESEARCH AND DEVELOPMENT CENTER
AIR FORCE SYSTEMS COMMAND
WRIGHT-PATTERSON AIR FORCE BASE, OHIO 45433-6533

NOTICE

When Government drawings, specifications, or other data are used for any purpose other than in connection with a definitely Government-related procurement, the United States Government incurs no responsibility or any obligation whatsoever. The fact that the Government may have formulated or in any way supplied the said drawings, specifications, or other data, is not to be regarded by implication, or otherwise in any manner construed, as licensing the holder, or any other person or corporation; or as conveying any rights or permission to manufacture, use, or sell any patented invention that may in any way be related thereto.

This report is releasable to the National Technical Information Service (NTIS). At NTIS, it will be available to the general public, including foreign nations.

This technical report has been reviewed and is approved for publication.

Charles F. Buynak

CHARLES F. BUYNAK
Nondestructive Evaluation Branch
Metals and Ceramics Division

D. M. FORNEY, Chief
Nondestructive Evaluation Branch
Metals and Ceramics Division

FOR THE COMMANDER

Norman M Tallan

DR. NORMAN M. TALLAN, Director
Metals and Ceramics Division

If your address has changed, if you wish to be removed from our mailing list, or if the addressee is no longer employed by your organization please notify WRDC/MLLP, Wright-Patterson AFB, OH 45433-6533 to help us maintain a current mailing list.

Copies of this report should not be returned unless return is required by security considerations, contractual obligations, or notice on a specific document.

UNCLASSIFIED
SECURITY CLASSIFICATION OF THIS PAGE

REPORT DOCUMENTATION PAGE

Form Approved OMB No. 0704-0188

1a. REPORT SECURITY CLASSIFICATION UNCLASSIFIED	1b. RESTRICTIVE MARKINGS
2a. SECURITY CLASSIFICATION AUTHORITY	3. DISTRIBUTION / AVAILABILITY OF REPORT APPROVED FOR PUBLIC RELEASE DISTRIBUTION IS UNLIMITED
2b. DECLASSIFICATION / DOWNGRADING SCHEDULE	
4. PERFORMING ORGANIZATION REPORT NUMBER(S)	5. MONITORING ORGANIZATION REPORT NUMBER(S) WRDC-TR-89-4113
6a. NAME OF PERFORMING ORGANIZATION BOEING AEROSPACE COMPANY 6b. OFFICE SYMBOL (If applicable)	7a. NAME OF MONITORING ORGANIZATION WRIGHT RESEARCH AND DEVELOPMENT CENTER MATERIALS LABORATORY (WRDC/MLLP)
6c. ADDRESS (City, State, and ZIP Code) P.O. BOX 3999 SEATTLE WA 98124	7b. ADDRESS (City, State, and ZIP Code) WRIGHT-PATTERSON AFB OH 45433-6533
8a. NAME OF FUNDING / SPONSORING ORGANIZATION 8b. OFFICE SYMBOL (If applicable)	9. PROCUREMENT INSTRUMENT IDENTIFICATION NUMBER F33615-88-C-5404
8c. ADDRESS (City, State, and ZIP Code)	10. SOURCE OF FUNDING NUMBERS

PROGRAM ELEMENT NO.	PROJECT NO.	TASK NO	WORK UNIT ACCESSION NO.
63211F	3153	00	06

11. TITLE (Include Security Classification)
COMPUTED TOMOGRAPHY OF THERMAL BATTERIES & OTHER CLOSED SYSTEMS

12. PERSONAL AUTHOR(S)
RICHARD H. BOSSI

13a. TYPE OF REPORT	13b. TIME COVERED	14. DATE OF REPORT (Year, Month, Day)	15. PAGE COUNT
INTERIM	FROM AUG 88 TO JUN 89	DECEMBER 1989	53

16. SUPPLEMENTARY NOTATION

17. COSATI CODES			18. SUBJECT TERMS (Continue on reverse if necessary and identify by block number)
FIELD	GROUP	SUB-GROUP	
11	06		Closed Systems /Dual Energy /Inspection
11	03		Computed Tomography (CT) /Radiography /Gear Drive
			Nondestructive Evaluation (NDE) /X-Ray /Hydraulic Actuator

19. ABSTRACT (Continue on reverse if necessary and identify by block number)

Under a preliminary testing task assignment of the Advanced Development of X-ray Computed Tomography Applications program, computed tomography (CT) has been applied to several types of closed system components. For this task, closed system components were defined as components which were closed structurally such that the interior could not be inspected except by penetrating radiation. The primary testing emphasis was with thermal batteries. The units are hermetically sealed with a number of internal components and materials whose proper assembly and orientation is essential for successful operation. In addition to thermal batteries, several other mechanical and electromechanical closed systems were examined, including: missile and rocket launch secure and enable systems, and aircraft mechanical actuators and drive subsystems.

(Con't)

20. DISTRIBUTION / AVAILABILITY OF ABSTRACT	21. ABSTRACT SECURITY CLASSIFICATION	
☒ UNCLASSIFIED/UNLIMITED ☐ SAME AS RPT. ☐ DTIC USERS	UNCLASSIFIED	
22a. NAME OF RESPONSIBLE INDIVIDUAL Charles F. Buynak	22b. TELEPHONE (Include Area Code) 513 255-9802	22c. OFFICE SYMBOL WRDC/MLLP

DD Form 1473, JUN 86 *Previous editions are obsolete.* SECURITY CLASSIFICATION OF THIS PAGE

UNCLASSIFIED

19. (Con't)

Nine different CT systems were used for the scanning. Data from resolution and contrast sensitivity phantoms, developed for the program, were used to establish quantitative measures of imaging capability.

The results of the preliminary testing of thermal batteries concluded that digital radiography competes directly with film radiography for image quality and has superior throughput. In addition, CT scanning provided substantially more quantitative information on internal features such as cracking in cells and insulation; however, the economic incentive to have improved inspection capability is marginal. Battery failure analysis studies are aided by conventional CT and dual energy CT techniques, and should be studied further. The penetration and resolving power of CT systems on electromechanical and heavy duty aircraft mechanical closed systems was shown to be useful in the evaluation of important configuration features. In some cases, higher resolution CT is desirable. Applications in this area would be in prototype design or failure analysis.

Boeing Aerospace and Electronics

TASK ASSIGNMENT 2 - CLOSED SYSTEMS
(Preliminary Testing)
Interim Technical Report

for
Wright Research and Development Center
Contract #F33615-88-C-5404

Prepared by: John L. Cline
Checked by: Benjamin W. Knutson
Richard H. Bossi
Supervised by: James M. Nelson
Approved by: John E. Shrader

Final - 11//89

LIMITATIONS

DISCLAIMER

The information contained in this document is neither an endorsement nor criticism for any X-ray imaging instrumentation or equipment used in this study.

ABSTRACT

Under a preliminary testing task assignment of the Advanced Development of X-ray Computed Tomography Applications program, computed tomography (CT) has been applied to several types of closed system components. For this task, closed system components were defined as components which were closed structurally such that the interior could not be inspected except by penetrating radiation. The primary testing emphasis was with thermal batteries. The units are hermetically sealed with a number of internal components and materials whose proper assembly and orientation is essential for successful operation. In addition to thermal batteries, several other mechanical and electromechanical closed systems were examined, including: missile and rocket launch secure and enable systems, and aircraft mechanical actuators and drive subsystems.

Nine different CT systems were used for the scanning. Data from resolution and contrast sensitivity phantoms, developed for the program, were used to establish quantitative measures of imaging capability.

The results of the preliminary testing on thermal batteries concluded that digital radiography competes directly with film radiography for image quality and has superior throughput. In addition, CT scanning provided substantially more quantitative information on internal features such as cracking in cells and insulation; however, the economic incentive to have improved inspection capability is marginal. Battery failure analysis studies are aided by conventional CT and dual energy CT techniques, and should be studied further. The penetration and resolving power of CT systems on electromechanical and heavy duty aircraft mechanical closed systems was shown to be useful in the evaluation of important configuration features. In some cases, higher resolution CT is desirable. Applications in this area would be in prototype design or failure analysis.

Key Words

actuator
closed systems
computed tomography
digital radiography
dual energy
failure analysis
film radiography
gear drive
hydraulic actuator
inspection
nondestructive evaluation
thermal battery
X-ray

TABLE OF CONTENTS

TABLE OF CONTENTS- Concluded

APPENDICES **Page**

LIST OF FIGURES

LIST OF FIGURES - Concluded

1.0 INTRODUCTION

The goal of the Advanced Development of X-ray Computed Tomography Applications demonstration (CTAD) program is to evaluate inspection applications for which computed tomography (CT) can provide a cost-effective means of inspecting aircraft/aerospace components. The program is task assigned so that specific CT applications or application areas can be addressed in separate task assigned projects. This interim report is the result of a task assignment study. Under the program, candidate hardware is selected for testing that offers potential for return on investment (ROI) for the nondestructive evaluation system and operation. Three categories of task assignment are employed in the program: 1) preliminary tests where a variety of parts and components in an application area are evaluated for their suitability to CT examinations for their inspection; 2) final tests where one or a few components are selected for detailed testing of CT capability to detect and quantify defects; and 3) demonstrations where the economic viability of CT to the inspection problem are analyzed and the results presented to government and industry.

X-ray computed tomography (CT) is a powerful nondestructive evaluation technique that was conceived in the early 1960's and has been developing rapidly ever since. CT uses penetrating radiation from many angles to reconstruct image cross sections of an object. The clear images of an interior plane of an object are achieved without the confusion of superposition of features often found with conventional film radiography. CT can provide quantitative information about the density and dimensions of the features imaged.

Although CT has been predominantly applied to medicine, industrial applications have been growing over the past decade. Medical systems are designed for high throughput and low dosages specifically for humans and human sized objects. These systems can be applied to industrial objects that have low atomic number and are less than one-half meter diameter. Industrial CT systems do not have dosage and size constraints. They are built in a wide range of sizes from the inspection of small jet engine turbine blades using mid-energy (hundreds of keV) X-ray sources to the inspection of large ICBM missiles requiring high (MeV level) X-ray energies. Industrial CT systems generally have much less throughput than medical systems. The CTAD program utilizes a wide range of CT systems, both medical and industrial. CT systems offer source energy levels in roughly three categories: low (up to 150 kV), medium (up to 420 kV) and high (2 to 16 MeV).

1.1 Scope

This Task Assignment, designated "Task 2 - Closed Systems", is a preliminary testing task in the area of closed systems. This report discusses the components selected for testing, the results of testing and the conclusions drawn. Closed systems include components that are assembled such that their internal configuration cannot be evaluated without disassembly or the use of penetrating radiation. In the execution of this task, comparison tests using the same part were performed on a variety of CT systems. Studies on five categories of closed systems are contained in this report. They include: 1) thermal batteries, 2) safe and arm devices, 3) command signal decoder, 4) aircraft gear drive assembly and 5) aircraft hydraulic slat actuator.

1.2 Objectives

The objectives of closed systems evaluation were to: 1) establish a database of CT test inspections on selected closed system components; 2) evaluate the technical relevance, or usefulness, of applying CT to each of the selected components; 3) assess the potential economic incentives for utilizing CT inspection; and 4) assess candidates for follow-on evaluations. To assist in accomplishing these objectives, a variety of CT machines were utilized to assess the capability of different machine designs to meet inspection criteria.

1.3 Closed systems

Closed systems, such as thermal batteries, mechanical assemblies and electromechanical devices, represent a classification of aircraft/aerospace components that are suited to CT inspection technology because of their generally compact size, the opaque nature of their enclosures and the numerous internal elements that are assembled to make a precise unit. The elements within each closed system require inspection for a variety of reasons. Inspection of a closed system component during prototype development would allow verification of engineering design and component functionality, and evaluation of potential failure mechanisms prior to full-scale production. In-line, or off-line production inspection would provide verification of manufacturing quality control. Adequate nondestructive inspection of failed closed system components would provide valuable insight into the failure mechanism.

Presently little or no post-assembly nondestructive evaluation is performed on closed systems because of the inability to resolve internal details. Functional testing and occasionally film radiography are the usual testing procedures. CT testing has a particular advantage for complex systems because the image is obtained without the superposition of features that occurs in film radiography.

2.0 TEST PLAN

The Task 2 test plan called for the acquisition of test samples, CT scanning at a variety of facilities and evaluation of data. The primary interest was with thermal batteries; other mechanical and electromechanical devices were evaluated as a secondary consideration.

2.1 Part Selection

The primary selection rationale of closed system parts was based on the inadequacy of current NDE techniques. Other selection rationale included the component criticality, cost of the unit and the production rate. Figure 2.1-1 has a rating definition for component criticality. Figure 2.1-2 provides a value listing of test components selected for study in this task assignment.

Mission Critical:
Success of the mission (including human survival) is directly linked to the faultless operation of the component. Risks include high cost payloads, and human life. Cost of the component is Figured in with the success of the mission. Using CT for inspection may provide a very high payback.

Mission Essential:
Proper operation is essential, however, it is backed up by a redundant System which reduces criticality. Cost of the component,inspection and labor may be Figured in with some percentage of the mission success. The use of CT for inspection may provide a very high payback.

High Reliability:
High reliability is desired when failure of the component will not necessarily cause the mission to fail and it is backed up by several redundant Systems. Cost of the component is nominal and it is replaced without too much trouble. The use of CT for inspection is questionable.

Reliable:
Nominal reliability is desired and expected; however, failure of the component will minimally affect the mission and will not be a major issue. Redundancy and low replacement cost do not justify the use of CT for inspection purposes.

Figure 2.1-1 Component criticality rating

All test parts are given part identification (PID) numbers for logging in the CTAD parts database. Thermal batteries are given the code 0201XX. Other closed systems are coded as 0202XX. In this document, thermal batteries are referenced by the last three digits of the PID number, i.e., 101, 201, etc.

2.2 Schedule

Nine Industrial Computed Tomography (ICT) inspection facilities were used during the task assignment. The schedule of all tests and visits, by location and date, is given in Figure 2.2-1. Two days of scanning per visit was average and often additional scanning data were gathered without Boeing in attendance. Time and Material subcontracts were established with each of the commercial CT facilities. Additionally, several government-owned CT facilities provided scans at no cost to the contract. The NASA Marshal Space Flight Center (MSFC) provided scans using the ACTIS CT system on thermal batteries and CT standards, and a multiple, contiguous-slice, scan series on the gear drive assembly. Aerojet provided scans of the gear drive assembly, actuator, and a thermal battery using the Air Force ARNIS I system.

2.3 CT systems Characteristics and Performance

The CT systems used have been arbitrarily assigned letter name for designation. Figure 2.3-1 lists the performance measurements for eight of the nine CT systems (performance measurements were not made with the medical CT system). The measurements compare the ability to image a steel/acrylic line pair resolution phantom and the signal to noise in an aluminum phantom. To a first approximation, the data is meant to indicate the general resolution and signal/noise capability of the images obtained from the designated systems. The noise and resolution data is only a rough approximation because actual images may be obtained at different slice widths, fields of view and integration times than those used for the data in Figure 2.3-1. The standards used to obtain the data are described in Appendix A.

This closed systems task assignment often compares the performance of digital radiographic and computed tomographic capability of CT systems to conventional film radiographic inspection used presently. Appendix B provides an explanation of the three types of X-ray imaging techniques: film radiography, digital radiography and computed tomography.

Component	Cost	Replacement Importance
Thermal Battery	$200 to $4000	Full Range
Type A	High	Mission Critical
Type B	Average	Mission Essential
Type C	Average	High Reliability
Type D	Low	Reliable
Safe and Arm Device	$35,000	Mission Critical
Command signal Decoder	$200,000	Mission Essential
Aircraft Gear Drive Assembly	$25,000	High Reliability
Aircraft Hydraulic Actuator	$10,000	High Reliability

Figure 2.1-2 Value of test components

Location	1988			1989				
	Oct	Nov	Dec	Jan	Feb	Mar	Apr	May
ARACOR-LAMDE (Sunnyvale, CA)	10					28		
BIR - RADAPT II (Lincolnshire, ILL.)	24							
GE - XIM 3 (Cincinnati, OH)	27							
NASA MSFC-ACTIS (Huntsville, AL)		14				31		
SMS - 101B (Austin, TX)		21			28			27
EG&G - SMS 201 (Cape Canaveral, FL)			15					
GE XIM 6 and GE ICT (Cincinnati, OH)						27		
Aerojet - ARNIS 1 (Sacramento, CA)							10	

Figure 2.2-1 Testing Schedule

Scan Conditions				Results						
				Spatial Resolution: Steel Std.						
				Field +	% Modulation				Signal to Noise Al Std. (Center)	Average Cost per Image
System	Energy KeV/mA	Slice Thickness (mm)	Scan Time (min.)	of View (mm)	0.5 Lp/mm	1 Lp/mm	2 Lp/mm	4 Lp/mm		
A	420/4.0	1.5	30	60	—	55	0	0	17 (1)	$150
		15							73 (1)	
B	420/3.0	0.25	90	50	—	85	50	4	6 (1)	$300
		0.10	11		—	75	33	3		$ 65
		0.10	4.5		—	70	30	—		$ 30
C	300/5.0	1.0	12	80	—	46	10	0	11 (1)	$125
									49 (2)	
D	420/3.0	0.25	1.5	64	—	58	20	0	25 (2)	$ 15
E	420/3.0	0.25	0.5	64	—	57	7	0	4 (1)	$ 8
F	420/ 3.0	0.25	2.0	64	—	43	6	0	* *	$ 15
H	420/4.0	5.0	16	70	—	8	2	0	63	N/A
	2000	3.0	8	100	50	4	0	0	69	
I	2000	5.0	8	150	49	4	1	0	57	N/A

+ Field of view setting for resolution measurements only
* * Data Unavailable
(1) Al Noise Standard 5.5" dia.
(2) Al Noise Standard 2.75" dia.

Figure 2.3-1 CT System performance data

3.0 COMPONENT TESTING AND RESULTS

3.1 Category 1 - Thermal Batteries

Thermal batteries are used in a variety of aerospace applications to provide a one-time, on-demand source of electrical power with a very long shelf life. Boeing uses thermal batteries in the Air Launch Cruise Missile (ALCM), Sea Lance, Inertial Upper Stage (IUS), and the Short Range Attack Missile (SRAM II). Military aircraft utilize thermal batteries for ejection seat operation as well. Thermal battery use and readiness in flight vehicles is generally mission critical and failure can be catastrophic.

Thermal batteries, in general, are high-quantity, relatively low-cost items with a relatively high (on the order of 1 to 5 percent) rejection rate. They are hand assembled and quality control is essential to assure proper assembly. Reliability is typically 0.9995, verified by lot sampling. Radiographic inspection methods are used, but generally are not capable of adequately discerning all defects of interest and require intensive review.

A total of 11 thermal batteries were inspected during the test period. Eight batteries, in an assortment of sizes, were provided by Catalyst Research. Two intentionally flawed, quality control training batteries were supplied by Eagle Picher, and one fired battery was provided by the SRAM II program (Boeing). Figure 3.1-1 provides brief information about each battery, including its function, cost criticality (A through D - Figure 2.1-2), imaging goals, and results by individual site or CT system.

3.1.1 Hardware Description

A generic thermal battery, shown in Figure 3.1-2, consists of a stack of disk-shaped cells inside a hermetically-sealed metal can. Each cell consists of a metallic cathode, a fusible salt electrolyte, a metallic anode, a heat pellet, and an insulator. Electropotential difference between the cathode and the anode determines the voltage of each cell. The cells are stacked and connected by wires running along the outside of the stack to supply sufficient voltage to meet the battery specification. Because the electrolyte is a solid salt at room temperature, the degradation of thermal batteries with time is extremely low; shelf life generally exceeds ten years.

The battery is activated by supplying sufficient heat, supplied by igniting a pyrotechnic material such as potassium perchlorate, to melt the electrolyte. To achieve fast activation times, the heat source is usually built into the cell structure. A pyrotechnic (fuse) paper is either wrapped around the outside of the cell stack or inserted into a hole through the center of the cell stack. This pyrotechnic rod, or sleeve, is ignited on demand by either an electrically activated squib or a mechanically activated percussion cap. In general, the activation life of the thermal battery is limited by the ability to keep the electrolyte molten.

Component	Function	Cost $	(A is top) Criticality	Imaging Goals/Rqmt's	CT Systems	CT Ability	Payoff Potential
T/B # 101 Tab Mount	Air to Air Missile	100-300	B	• View Fuse Contact • Individual Screens	A, D	Fair	Unknown
T/B #102 Small 3 pin w/primer	Electronic Countermeasure	100-300	B	• X-ray highly difficult • Cell structure, lead attach.	C, D	Fair	Unknown
T/B #103 Hollow Bore	AAED High Tech Electronic Decoy	100-300	B	• Problem Battery • 2 diff. kinds cells • Fuse strip on ID	A	Fair	Unknown
T/B #106 Long - 8 terminals	Amraan Seeker - Guidance	100-350	B	• X-ray difficult - parallax	B, H	Very Good	Unknown
T/B #107 A few known defects - 4 mounting feet	Anti-tank weapon	100	B	• Short Fuse train • Missing cell-Batt • Reversed cell # 3 • Bad (-) lead weld	A, B, H	Fair	Unknown
T/B #108 Large oval	ALCM	4000	A	• Wiring anomalies • Post-vibration test	B, H	Very Good	Unknown
T/B #109 Multiple Known defects	Air Deployed Swamp Mine	100-300	B	• Reversed cells • Missing cell parts • Double cell parts	A, B, C, D, E, F, H, I	Fair	Unknown
T/B # 110 Miniature	Re-entry Vehicle (Warhead)	2000	A	• 5% fab success • CAD-CAM • Bi-metal stripe status	D	Good	High
T/B #111 Large fired	Remotely Controlled - Torepdo	500	B	• Cell structure after firing	A, C	Good	Unknown
T/B #112 Large fired	Remotely Controlled - Torepdo	500	B	• To compare with fired battery	A, C	Good	Unknown
T/B #115 Fired-rough appearance	SRAM 2	100-300	B	• CT as alternative to disection	H	Good	Superior Failure Analysis

Figure 3.1-1 Battery information table

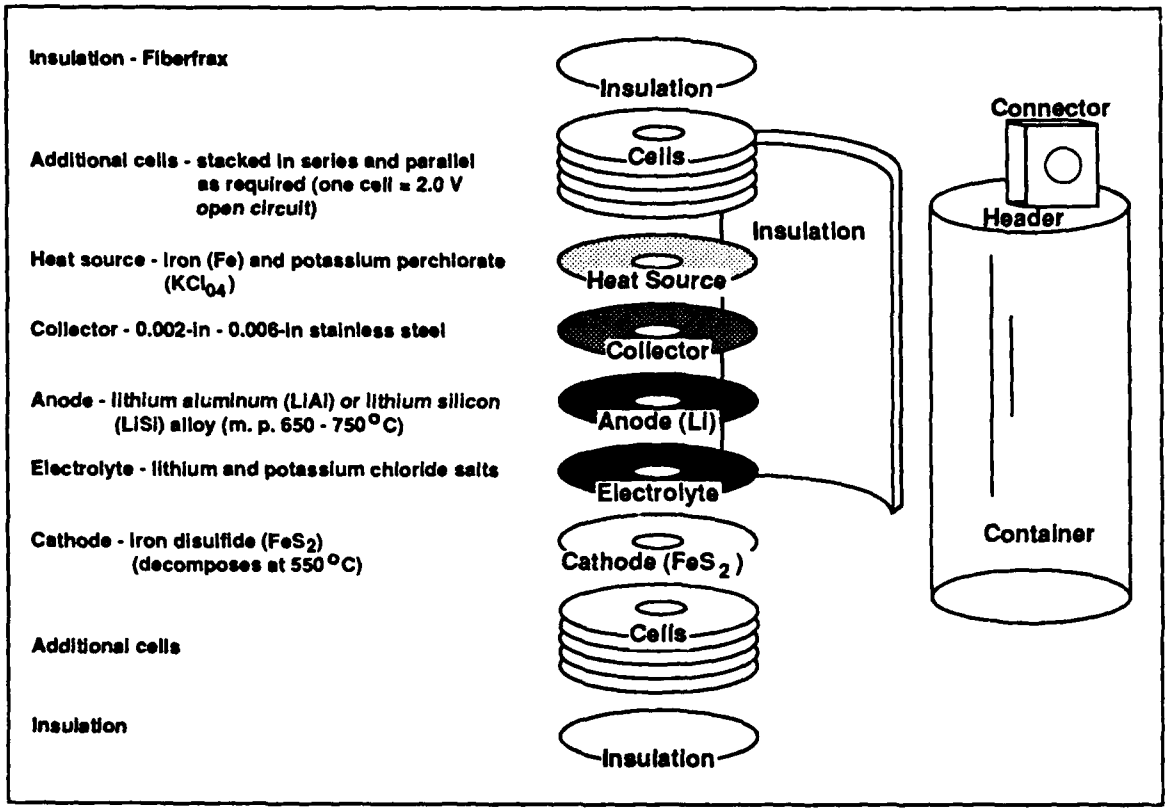

Figure 3.1-2 Details of thermal battery assembly

3.1.2 Inspection goals

The following is a list of items internal to a typical sealed thermal battery, which are presently verified, with greater or lesser degrees of success, by X-ray radiographic inspection methods:

* Proper number of cells
* Proper orientation of cells
* Proper location of cell components
* Good lead connections
* Unactivated squib
* Insulation under leads
* Insulation top, bottom, and around cell stack
* Fuse paper placement.

For most of these inspection goals, the primary criteria for an inspection technique is the ability to spatially resolve details of the battery along its axis.

Production acceptance inspection - which is often not 100 percent of the units - is only one need for radiographic inspection. Another valuable use for radiography is in the area of thermal battery failure analysis. A battery which fails a lot sampling test firing will make the remaining batteries of that lot suspect (typical lots for high production batteries range from 200 to 2000). If the mode of failure cannot be discovered from a

film radiograph and the sectioning of the failed battery, then the entire lot may be rejected. The following items, or conditions, can sometimes be seen in failed batteries:

* Improper cell orientation
* Missing cell component
* Missing lead insulation
* Location of short
* Improper wiring.

The consequence of a failed battery might result in considerable expense to the manufacturer for rework. Additionally, aircraft/aerospace program schedules and milestones can be seriously affected.

Several problems exist with current radiographic film techniques: parallax, the need for multiple exposures, and non-digital data format. Parallax resulting from the cone shaped X-ray beam intersecting the parallel plates of the battery causes the cells at the end of the battery to appear as ellipses, rather than lines. Because the ellipses overlap, resolving the details of each cell is difficult, except near the center of the radiograph. Because not all details can be seen on one radiograph, multiple radiographs of each part must be made with different orientations or different exposure times, increasing the cost of inspection. The number of cells for each battery must be counted by an operator from the X-ray image, which is time consuming and prone to human error.

CT has the potential to reduce or eliminate all of these problems. It is parallax free, and it is in digital format, so cell counting can be automated. By careful selection of slice location the number of different views required can be reduced and the large dynamic range of CT allows both low and high density features to be extracted from one exposure.

3.1.3 Test Conduct and Results

Batteries are constructed in a variety of shapes and sizes. The smaller batteries were tested on the smaller format CT systems, which also provided the highest resolution (2 to 4 lp/mm). The medium sized and large, high-energy CT systems could handle larger batteries and even batches of batteries, but offered moderate resolution (0.5 to 2 lp/mm). In a typical CT test scenero, digital radiographs (DR) are taken first and provide quick-look overall images from which specific CT slice locations can be indexed and subsequently scanned. CT slicing was taken primarily along the axial length of the battery. Multiple continuous slices across the batteries were also taken in several instances.

3.1.3.1 Special Interest Batteries

Batteries #101 and #103 were described by the manufacturer as difficult batteries to inspect. Battery #101 utilized a new-design thin screen mesh anode assembly which was extremely difficult to detect in the film radiograph. Battery #103 was unusual because it was constructed with a hollow core case and presented a problem with the ignition fuse strip down the center.

Battery #101 (P/N 40840), shown in Figure 3.1-3, is cylindrical, 4.2 cm (1.65 in) diameter by 13.5 cm (5.31 in) long, with a long external mounting tab. The battery has four terminals and utilizes a squib ignitor. Cells are 1.67 mm (0.066 in) thick. The objective of the scan was to see fuse contact down the center bore, and also to see the expansion screen layers within each cell. The film radiograph of the battery, shown in Figure 3.1-4, illustrates parallax problems at either end. Screen layers are difficult to see in the radiograph. Figure 3.1-5 is a DR taken on System D of the upper portion of the #101 battery. The DR has considerably more detail than the film radiograph. The dynamic range of the digitally obtained image allows better radiographic viewing than with film. Individual cells with the screen layer are evident. The DR view also provides a clear image of an unfired squib. Figure 3.1-6 is a CT cross-section view of one cell showing the screen mesh layer used in this battery's construction and the center bore fuse.

Battery #103 (P/N 40910), shown in Figure 3.1-7, is cylindrical, 6 cm (2.36 in) diameter by 7 cm (2.76 in) long, having a hollow opening down the center of the case. The manufacturer specified two important inspection issues: 1) difficult to see fuse strips, and 2) recognition of different cell types. The two types of cells were easily imaged and appear without the parallax problem associated with film radiography. Cell-to-cell density variations and cell separators are easily seen in the longitudinal CT slice as shown in Figure 3.1-8 from System A. In addition to longitudinal slices, a series of four axially normal slices, 1 mm (0.039 in) thick on 0.3 mm (0.012 in) centers, were taken over the width of one cell. Typical cell low to high (dark-to-light) image density variations were seen from CT slice to CT slice within an individual cell. Figure 3.1-9 shows a grouping of four contiguous slices with different shades representing different densities. An unexpected flaw was noticed in the last image and is shown in Figure 3.1-10. Although the crack does not present a problem to the operation of the battery, it is of imaging interest, particularly since the crack is detectable in a thin (0.5 mm (0.02 in)) CT slice. Had the crack been through an entire cell, potential for damaging electrolyte leakage would have existed. Fuse strips consisting of low density paper could be seen in this battery by adjusting the contrast range on the CT display.

3.1.3.2 Small Batteries

Batteries #102 and #110 are both less than 3.5 cm (1.38 in) in diameter and easily fit into the small format CT systems. Battery #102 (P/N 406340), Figure 3.1-11, is used as an electronic counter measures decoy power source. It contains different cell stacks and resolving the small (less than 0.6 mm (0.024 in.)) cells was important. The primer and lead attachments are of special interest because they often had problems in assembly. A longitudinal CT image from System D, Figure 3.1-12, shows the different cell stacks, leads and primer with excellent detail. Primer configuration is easily seen in a progression of CT slices taken through it. Lead attachments were imaged with CT, but it did not offer more resolution than conventional film radiography.

Battery #110 (P/N MC 3042), shown in Figure 3.1-13, is an ultra-small, high-voltage battery used in critical re-entry systems. It is expensive, hard to build, and it has a high mortality rate during construction. A fluoroscope is used to aid its construction by inspecting for reversed cells and associated features periodically during assembly. The battery was imaged on System D with sufficient detail to resolve less than 0.5 mm thick cells. Figure 3.1-14 is a DR. It shows the multiple cell stacks and the complicated

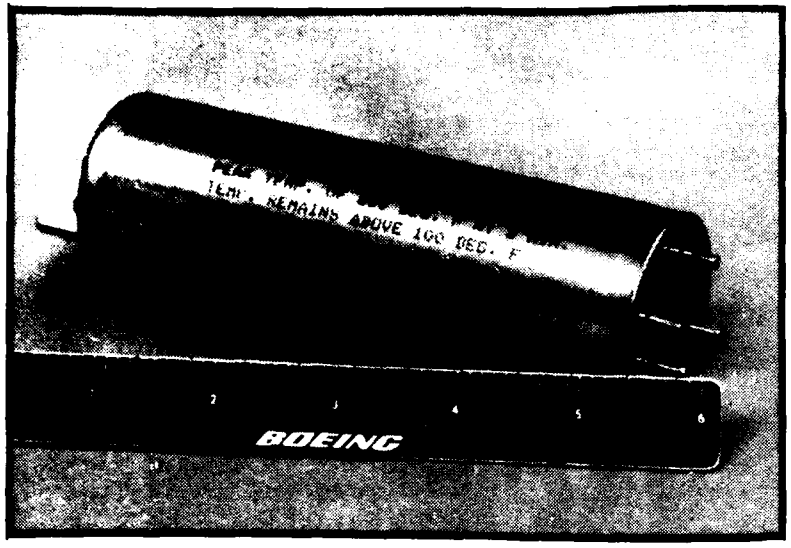

Figure 3.1-3 Tab mounted battery #101

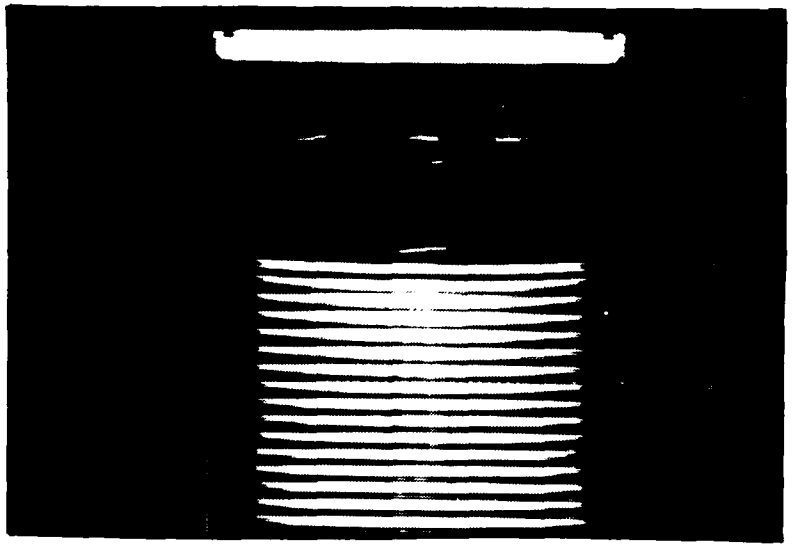

Figure 3.1-5 High detail DR of battery #101

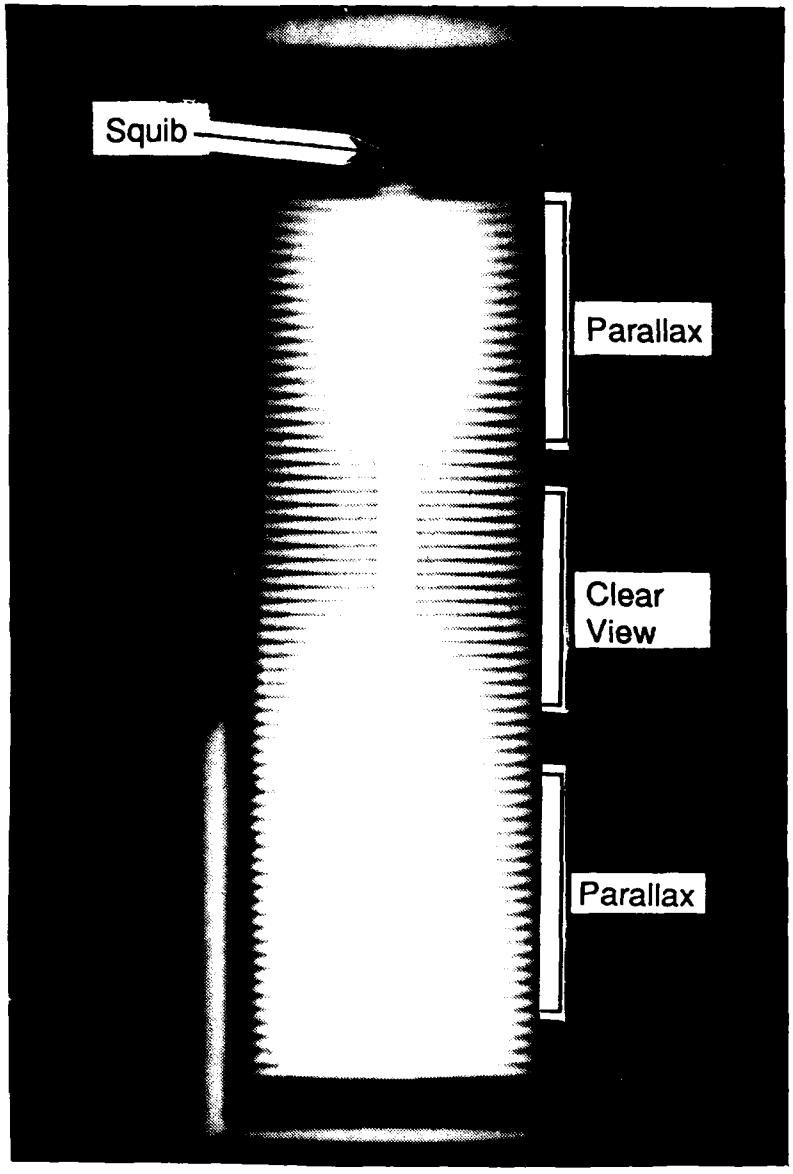

Figure 3.1-4 Film radiograph of battery #101

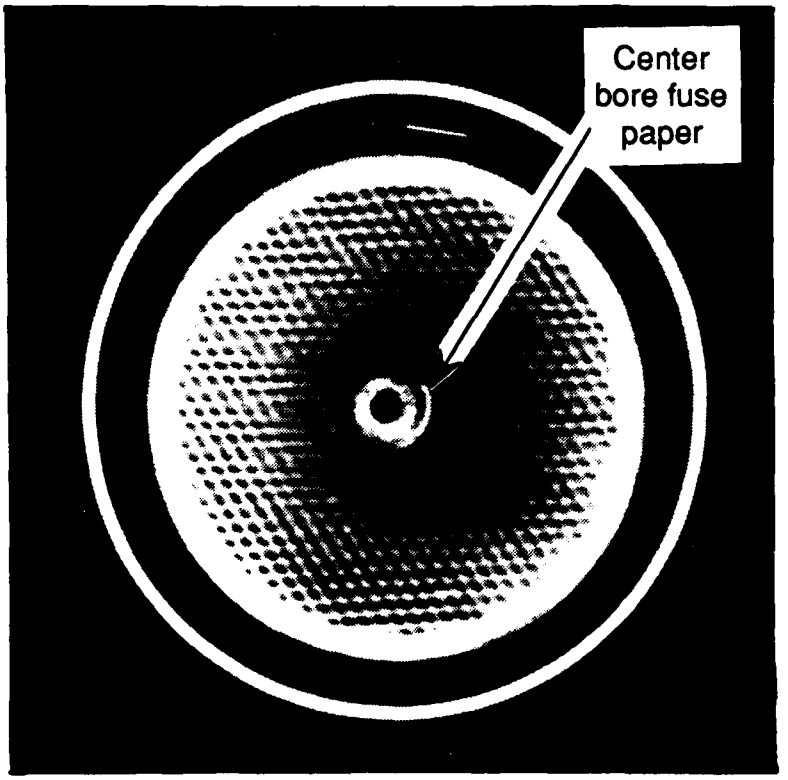

Figure 3.1-6 Screen cell of battery #101

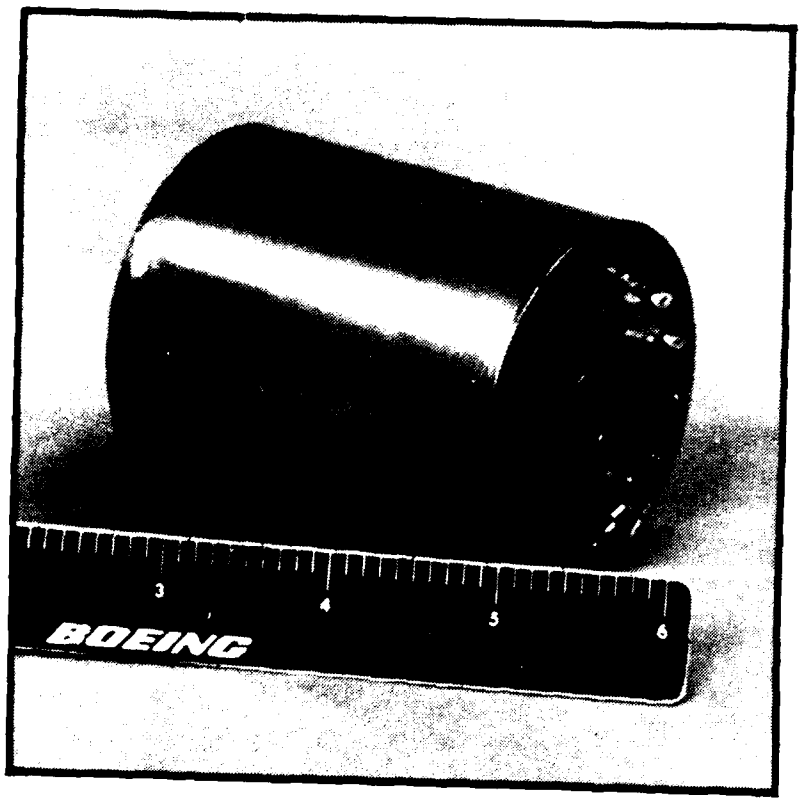

Figure 3.1-7 Hollow core battery #103

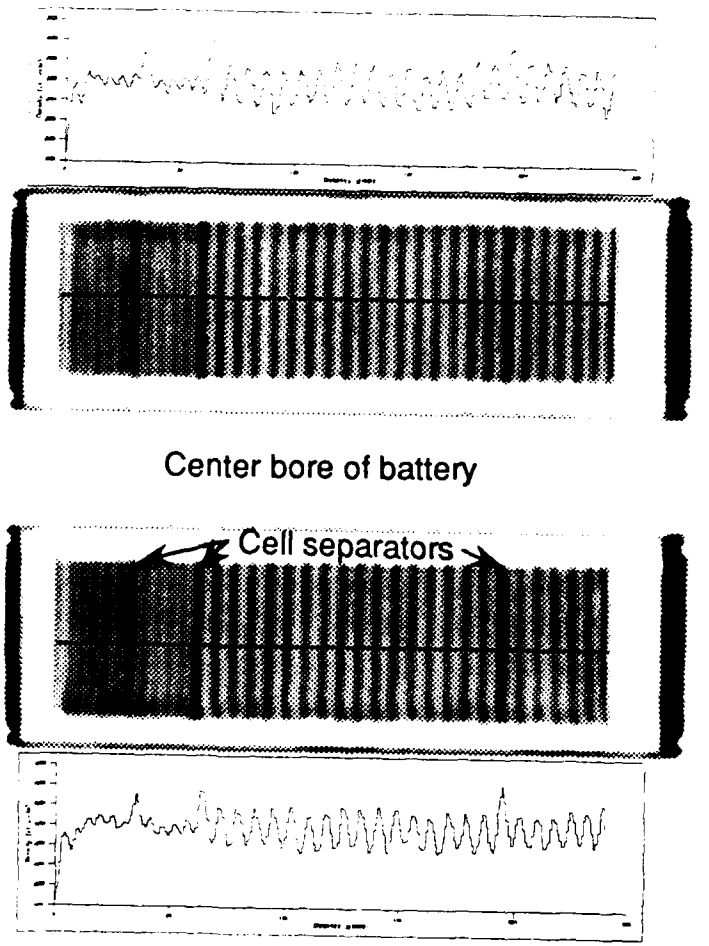

Figure 3.1-8 Line-out cell density plot of battery #103

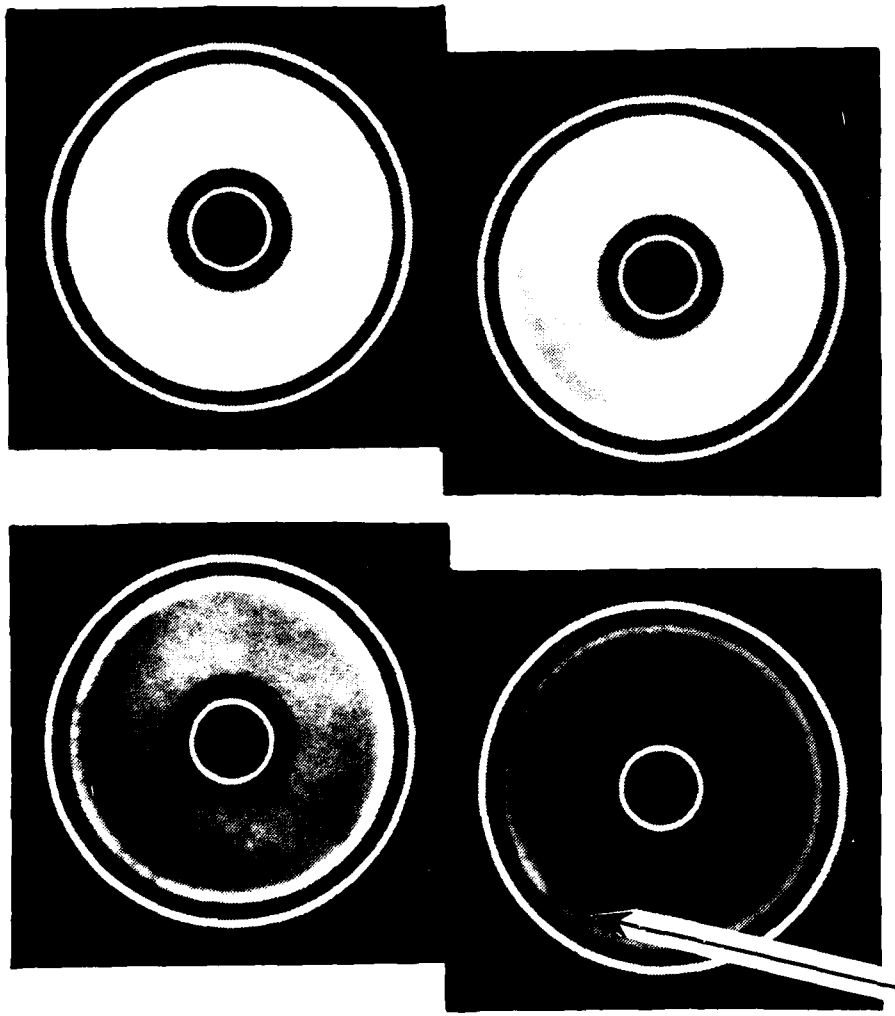

Figure 3.1-9 Multiple CT views over one cell of battery #103

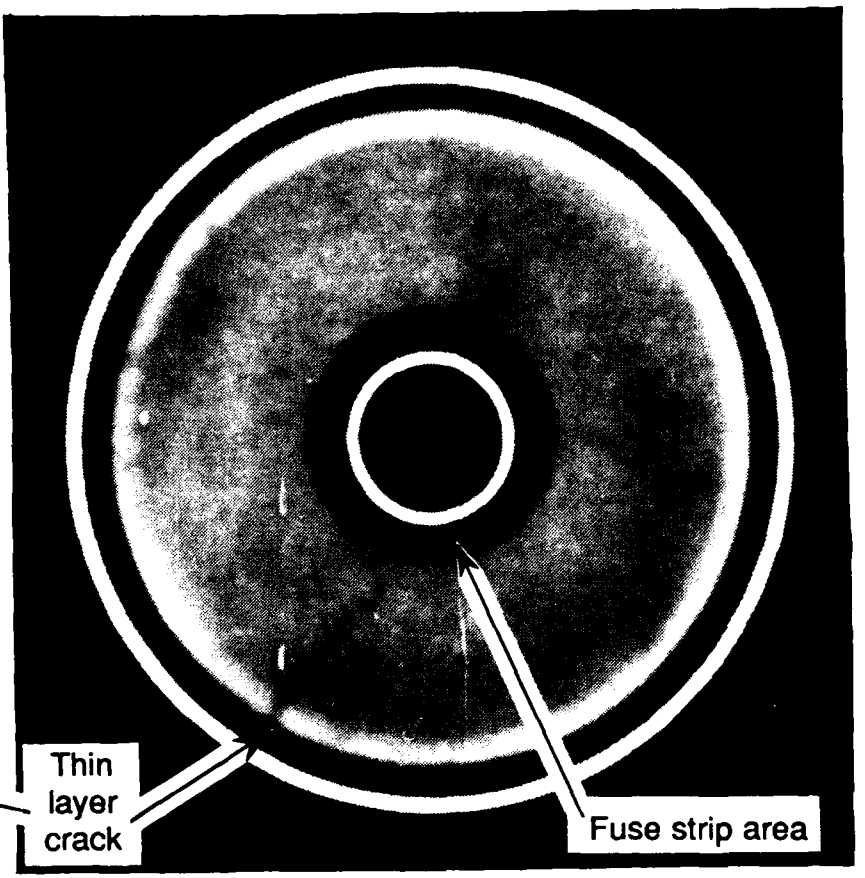

Figure 3.1-10 Cell with crack in battery #103

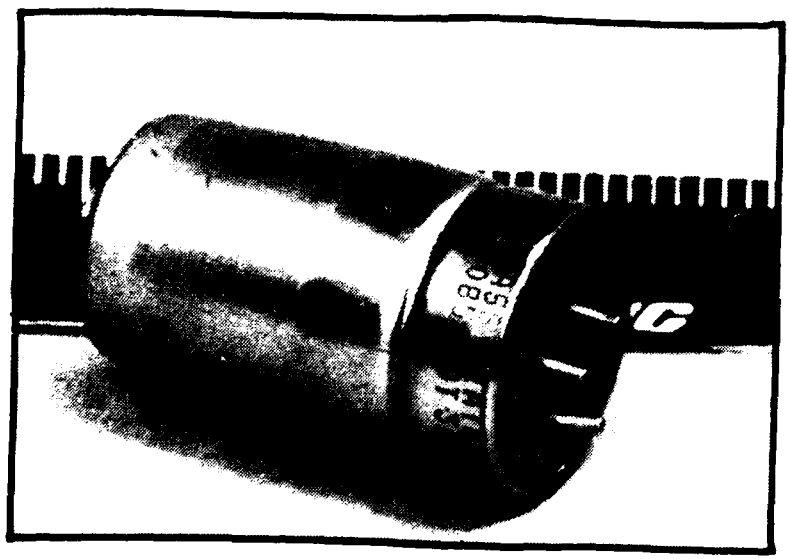

Figure 3.1-11 Small battery #102

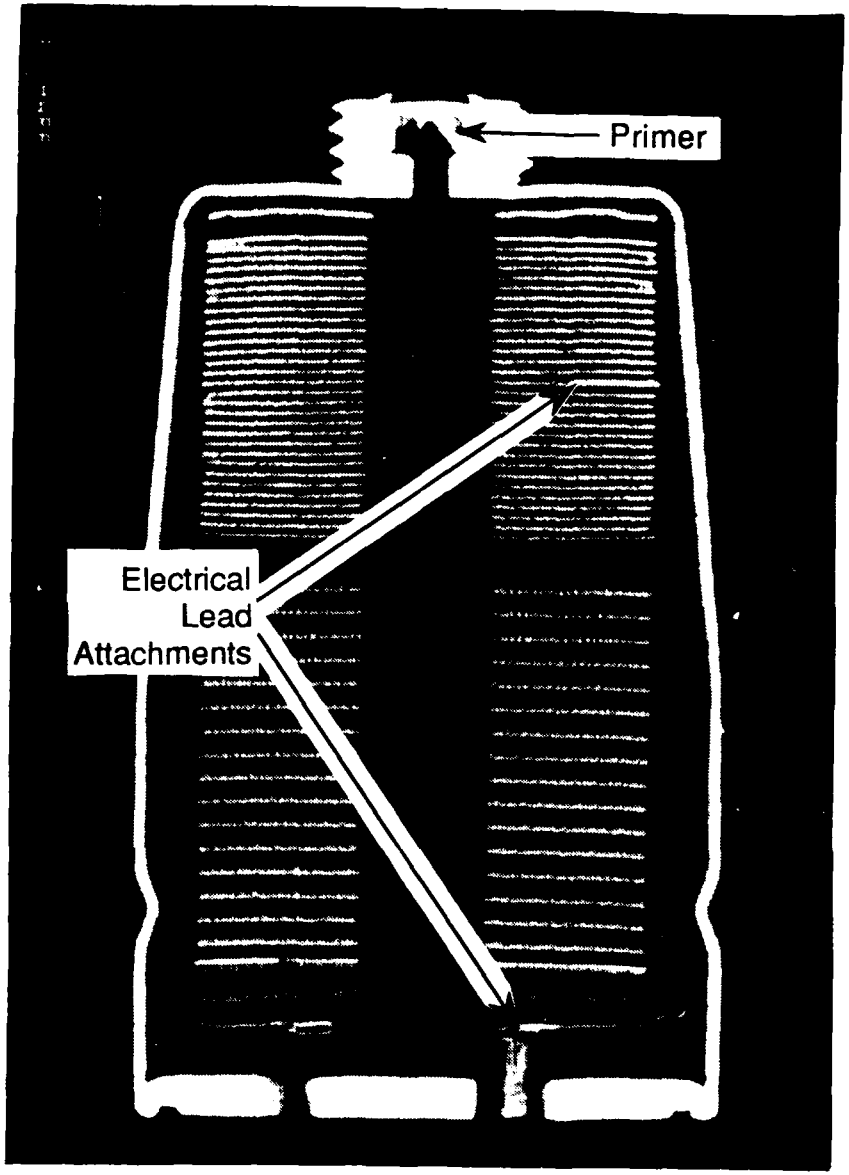

Figure 3.1-12 CT view of battery #102

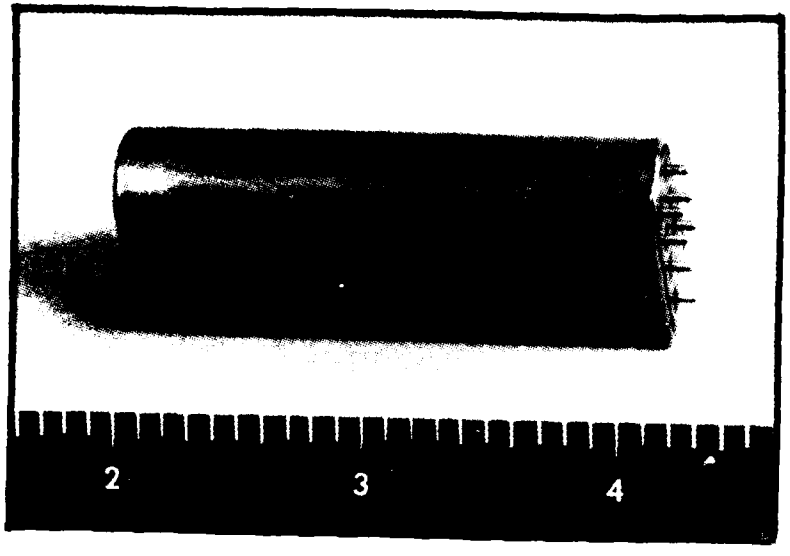

Figure 3.1-13 Miniature battery #110

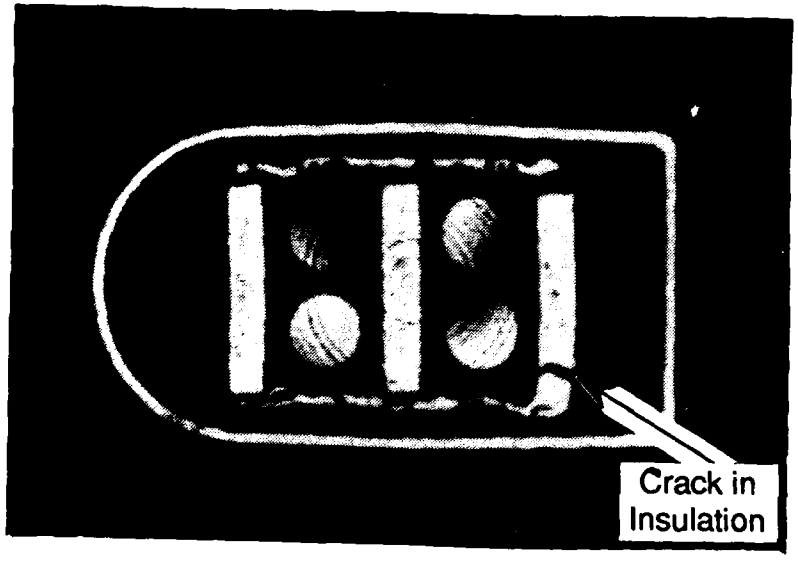

Figure 3.1-15 Axial view of battery #110 at indicated location

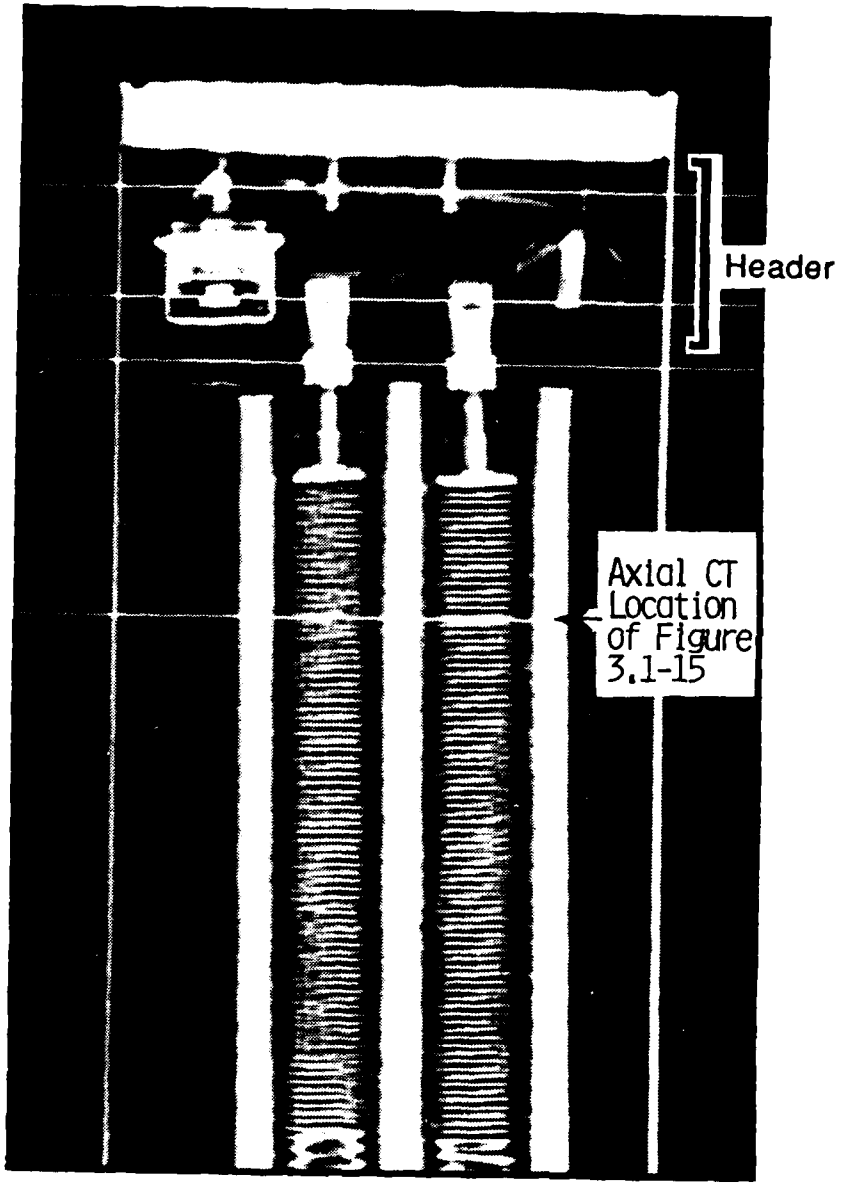

Figure 3.1-14 DR of miniature battery #110

wiring in the header. Cell detail in the DR is compromised by the screen resolution of the imaging system display monitor, and is not an improvement over film radiography in this instance. Figure 3.1-15 is a axial CT view taken midway down the battery, as indicated in Figure 3.1-14. It shows broken insulation, a potentially serious problem, which was previously undetected in the manufacturer's inspection.

3.1.3.3 Large Batteries

Battery #106 (P/N 202137), Figure 3.1-16, is 20 cm (7.87 in) long, requiring four radiographic exposures in order to limit parallax effects. In addition, the battery normally requires repeated turning to image lead pairs of the eight terminals in edge profile. Figure 3.1-17 is a film radiograph of battery #106. Blurring and distortion occurs at both ends due to parallax in the standard radiographic geometry. Battery #106 was inspected on System C. The heat paper placement and the insulation material were imaged the full length of the battery, as shown in Figure 3.1-18. It was also imaged on System H along with battery #108 in a multiple-battery batch inspection simulation mode, Figure 3.1-21. The CT images are definitive and parallax free.

Battery #108 (P/N 408020), Figure 3.1-19, was the largest battery tested. It supplies electrical power to the ALCM during launch. As with other large batteries, it requires multiple film radiographic exposures. A film radiographic image is shown in Figure 3.1-20. Battery #108 was imaged in a cross-axis view, on System H at 2 MeV, in a batch mode with three other batteries, shown in Figure 3.1-21. The three remaining batteries were imaged longitudinally in the same slice with impressive detail. A DR image of battery #108, taken on System B, is shown in Figure 3.1-22. The DR image shows greater detail than the equivalent conventional film radiograph, Figure 3.1-20, which did not cover the entire battery. A similar view, but in greater detail, was obtained with a longitudinal CT slice on System H, shown in Figure 3.1-23.

3.1.3.4 Flawed Batteries

Thermal batteries #107 and #109 were supplied with intentional flaws, and consequently were of particular interest. Battery #107 (P/N 12009), Figure 3.1-24, is medium size, cylindrical, and squib type, with four mounting feet and five terminals. The cell thickness is 1.35 mm (0.05 in), which is average. This battery has a missing cell and a reversed cell. It contains a short fuse train (paper on side), a bad spot weld on the negative lead, and a looped lead at the header. A series of film radiographs of the part were closely inspected for these anomalies. Only the missing cell and the reversed cell were visible.

Figure 3.1-25 is a System B DR of battery #107. The reversed cell was detected in the DR. The missing cell in the first half was easily detected by counting the number of cells on each side of the center section separator; 31 are on one side instead of 32. The other flaws were not discerned, as was the case with film radiography. Figure 3.1-26 is a longitudinal CT view using System H at 420 kVp. A CT image taken with a 2 MeV source on System H was not as detailed as the 420 kVp image. Unlike battery #109, detection of the reversed cell and other flaws did not improve with CT. This battery was also scanned on a medical CT machine, but the scan images are not included in this report. All cells were visible; however, beam hardening and streak

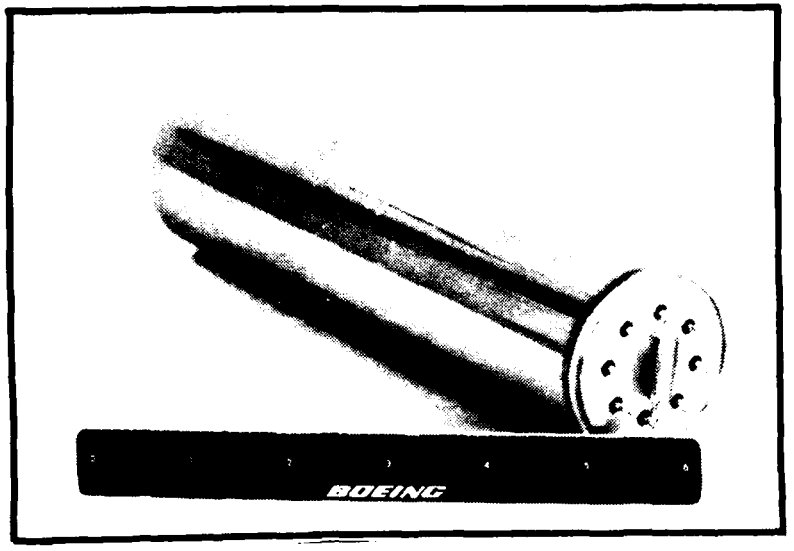

Figure 3.1-16 Long Battery (#106) with multiple connections

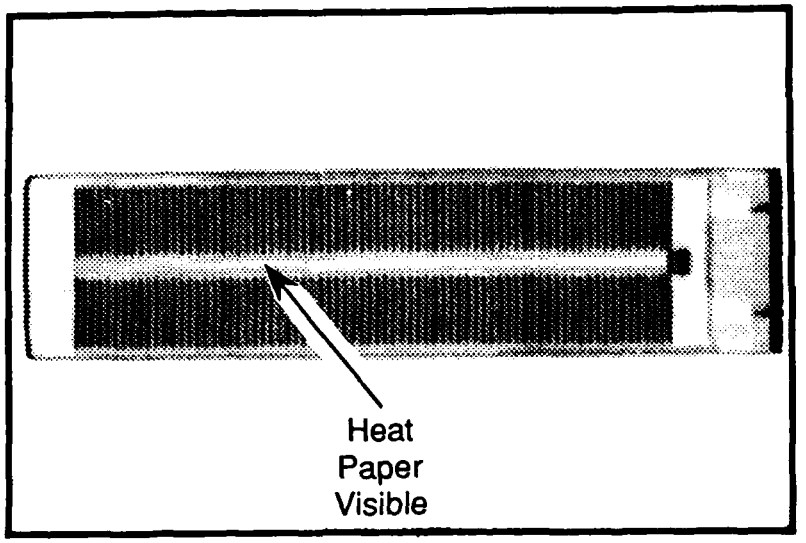

Figure 3.1-18 CT view showing heat paper in battery #106

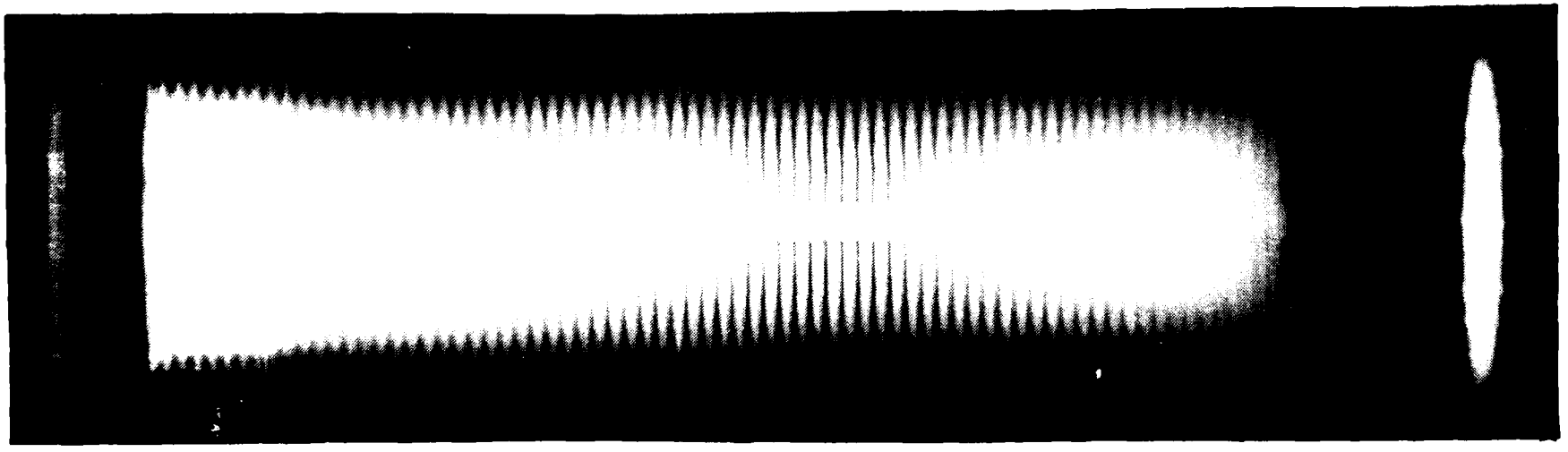

Figure 3.1-17 Film radiograph of battery #106

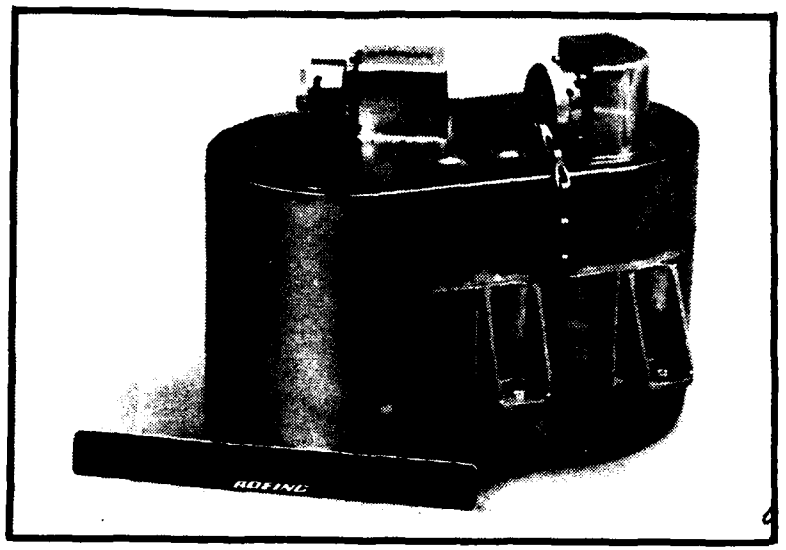

Figure 3.1-19 ALCM battery #108

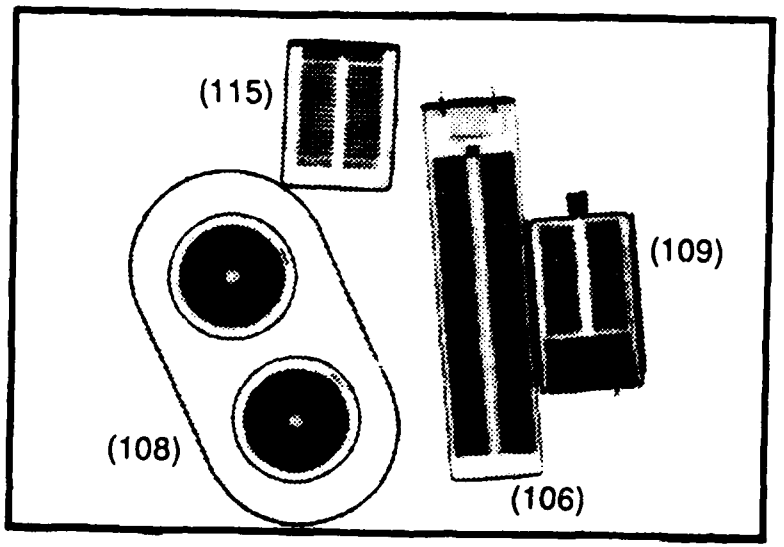

Figure 3.1-21 Multiple battery CT view (batch imaging) (#106, #108, #109, #115)

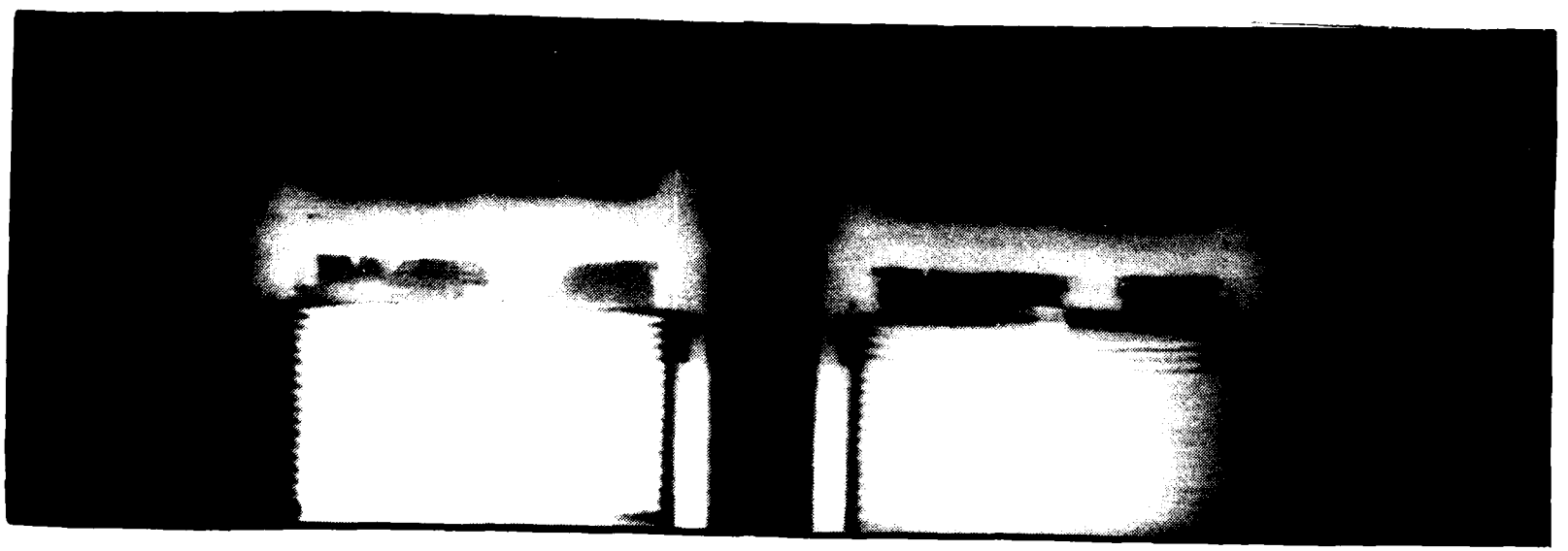

Figure 3.1-20 Limited view film radiograph of battery #108

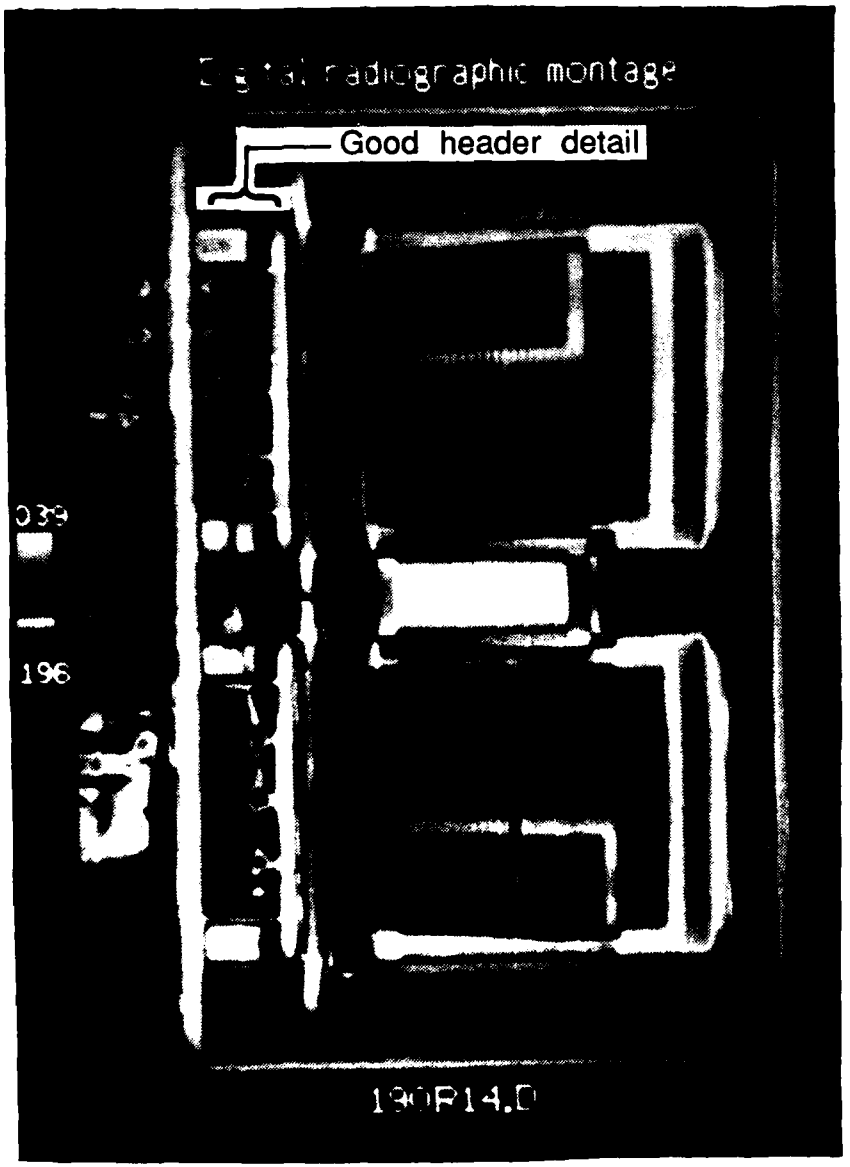

Figure 3.1-22 DR of battery #108

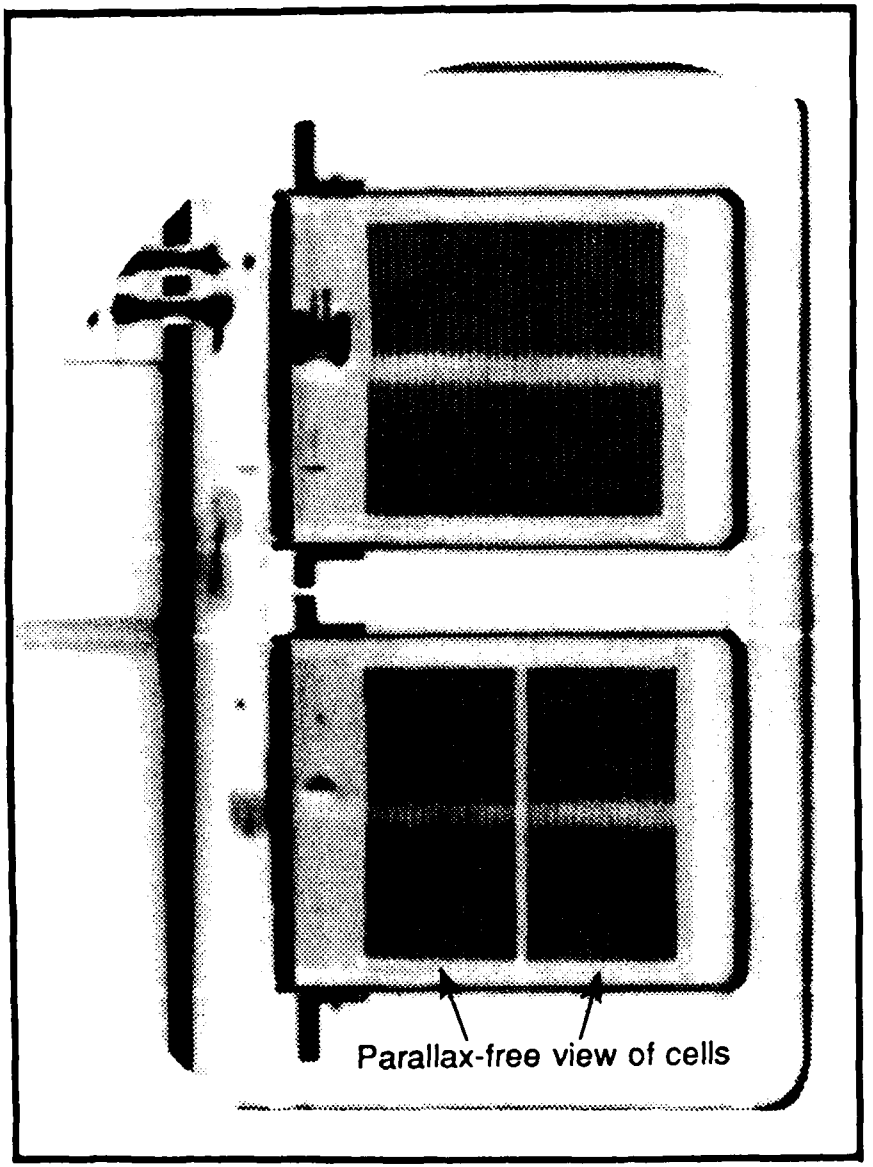

Figure 3.1-23 CT view of battery #108

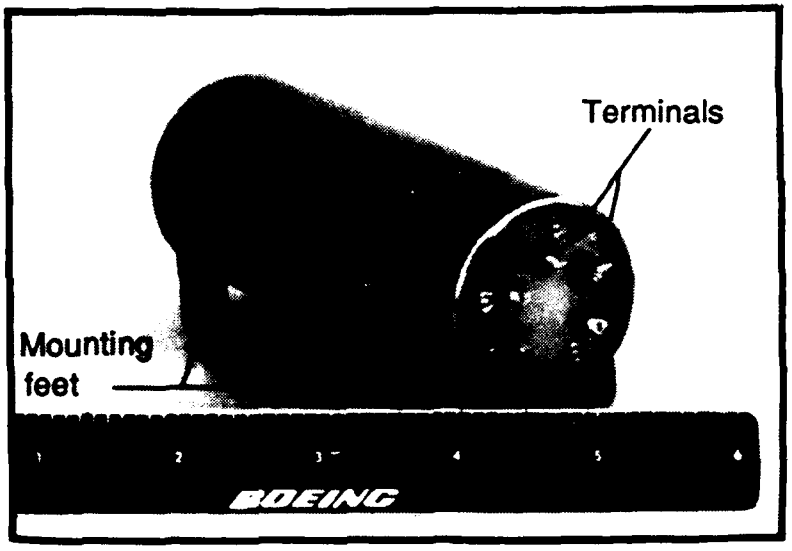

Figure 3.1-24 Defective battery #107

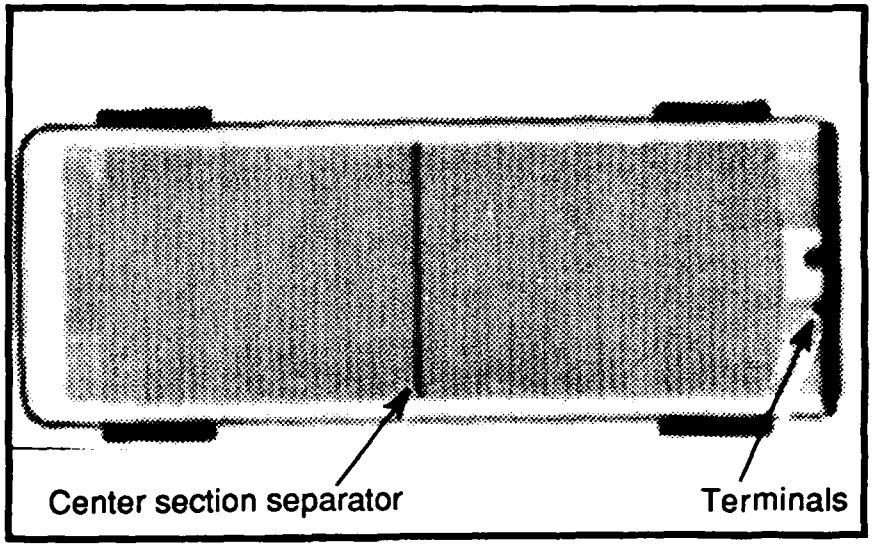

Figure 3.1-26 CT view of battery #107

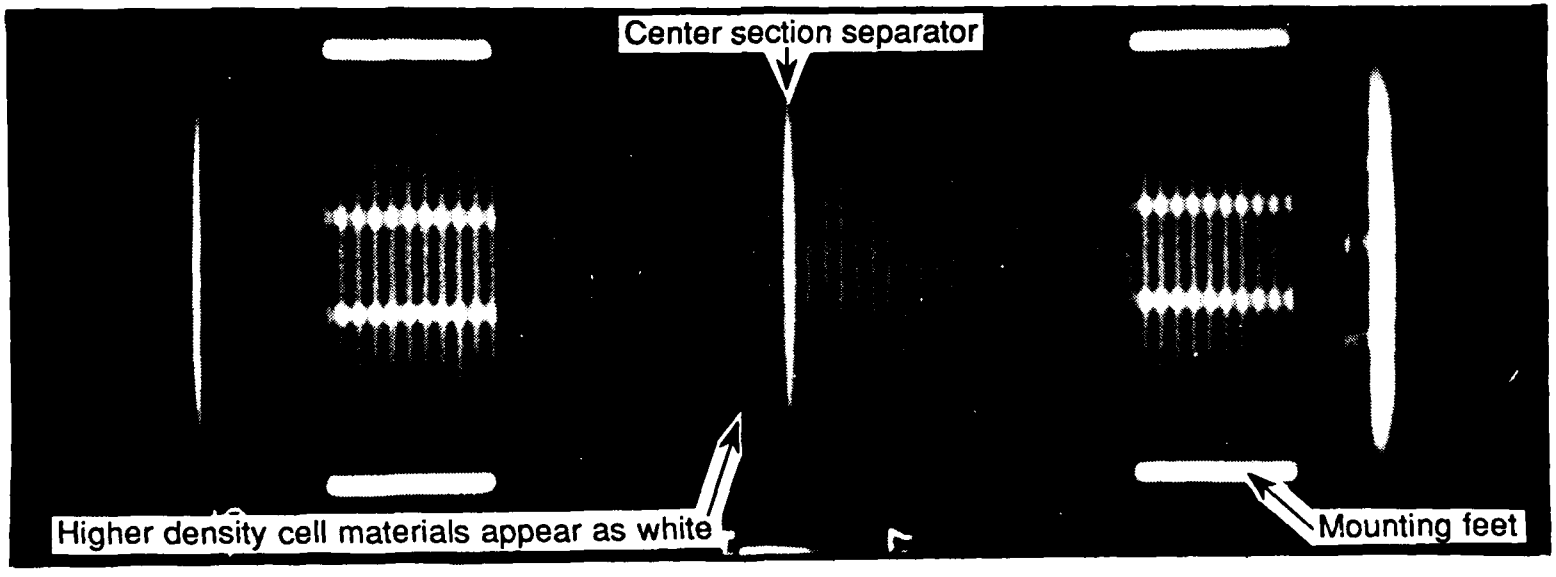

Figure 3.1-25 DR of battery #107

artifacts emanating from both ends of the battery were considerable with the medical system.

Battery #109 (S/N 12041) was chosen as the standard test battery for a round-robin series of inspections performed on nearly all CT systems visited. A photograph of this battery is shown in Figure 3.1-27. The battery contains six intentional flaws relating to different cells within the stack and was designed to train QA radiographers at detecting flaws. The flaws include: double electrolyte (cell #6), a missing electrode (cell #12), a reversed lithium electrode (cell #16), reversed FeS_2 and electrolyte (cell #20), missing lithium pellet (cell #26) and a double electrode (cell #30). (Note: first "cell" is not included in count.) All six battery flaws were detected on each of the CT systems to a greater or lesser degree. In general, the flaws were noted and annotated on hardcopy images.

Figure 3.1-28 is a System B longitudinal CT slice through two terminals, imaging the leads and lead connections. Figure 3.1-29 is a flaw annotated DR image (partial view) from System D. A System D CT image (partial) is shown in Figure 3.1-30. This CT view is of marginal quality because of the data limitations in reconstruction due to the limited (7.5 cm (2.95 in)) field of view employed. The density variations due to the anomalous cells are quite apparent in both the DR and CT. A System B image, Figure 3.1-31, shows the lower left hand portion of the battery with an annotated density plot which shows the correspondence of density variation in the image to four of the six anomalous cells that appear in this portion. Some apparent warpage and bending of the cells is also noticeable. Figure 3.1-32 shows a longitudinal CT view of battery #109 and a line density plot of both the top and bottom portions of the battery from System A. Specific anomalous cells are readily identified. Film radiographers can detect these anomalies in radiographs but even an unskilled observer can detect them using CT and density profiling.

3.1.3.5 Fired Batteries

Two batteries were obtained for testing to see if the effects of firing could be identified. Fired batteries, in general, appear much the same as before firing, but have somewhat warped and wavy cells. The squib or primer, however, always shows up altered due to firing.

Battery #112 (P/N 408890), pictured in Figure 3.1-33, is identical to a companion battery, #111, except that it is fired and #111 is unfired. Figure 3.1-34 is a longitudinal CT view showing a gradation of densities in each of the relatively thick (5 mm (0.2 in)) cells. Figure 3.1-35 is a System C CT view through the fired squib of battery #112. A battery firing may produce very little recognizable differences in the radiographic image of the cells. Figure 3.1-36 is a CT image of fired battery #112, showing little internal change except for cell slump. (Note: bottom of the battery is to the right.).

Dual energy CT scanning was tried in order to resolve subtle cellular changes due to firing. Dual energy inspection involves obtaining images at two effective energies and calculating the Compton and photoelectric effect. This may be accomplished by two methods: 1) taking two CT scans at different energies; or 2) utilizing two sets of detectors, front and back, where one set absorbs low energy and the other high energy. The second method was used on System A with careful calibration procedures to allow

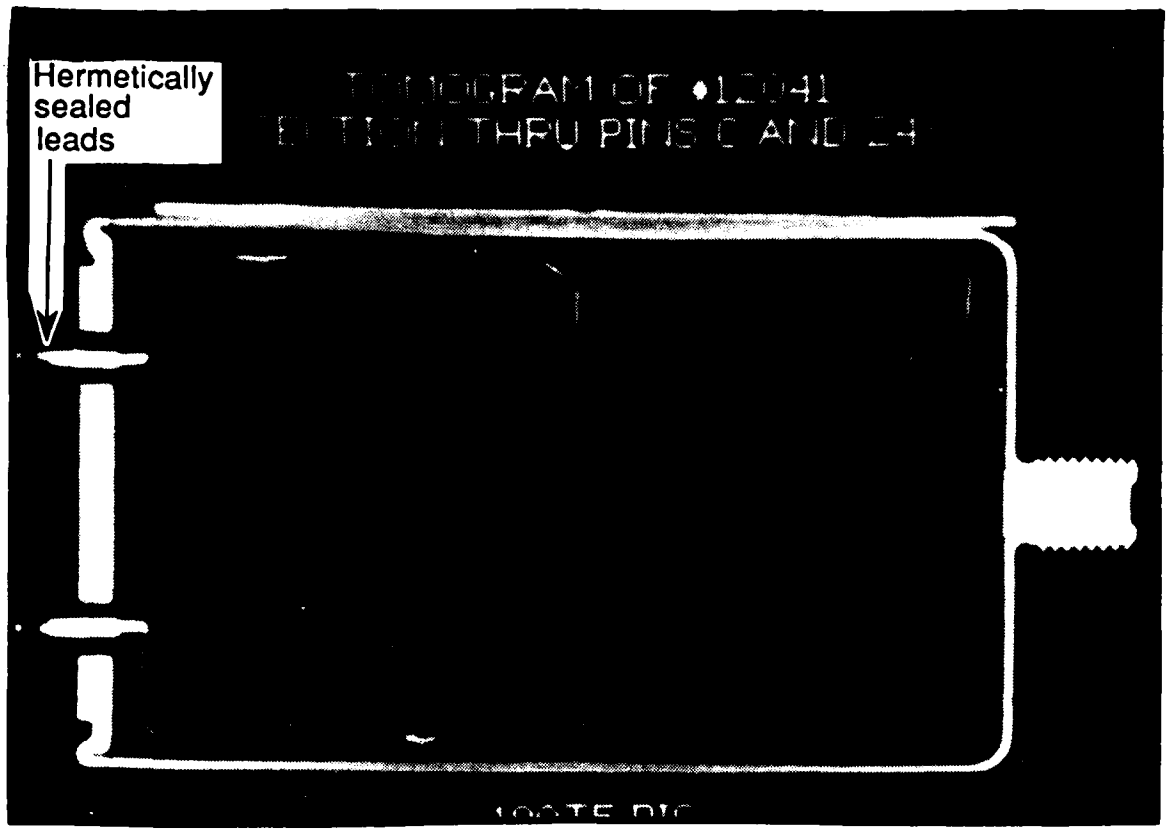

Figure 3.1-28 CT View of battery #109

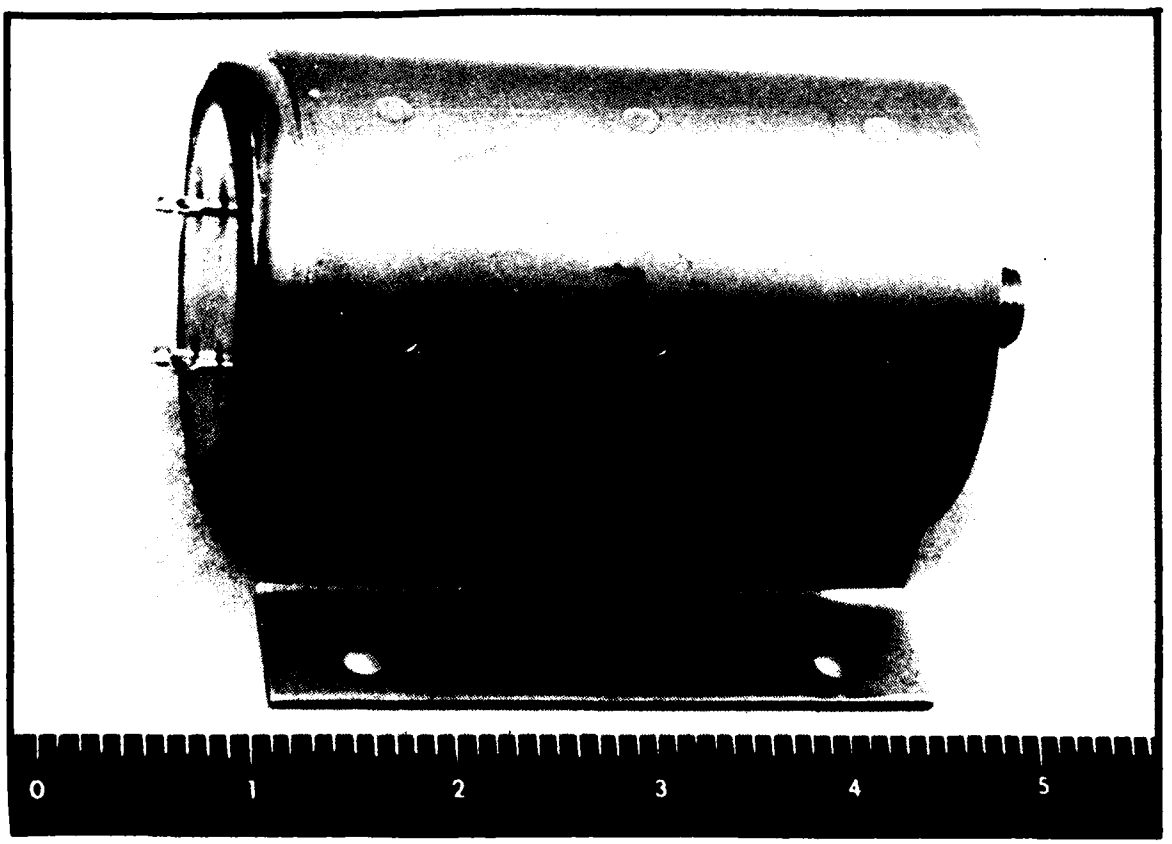

Figure 3.1-27 Multiple-fault battery #109

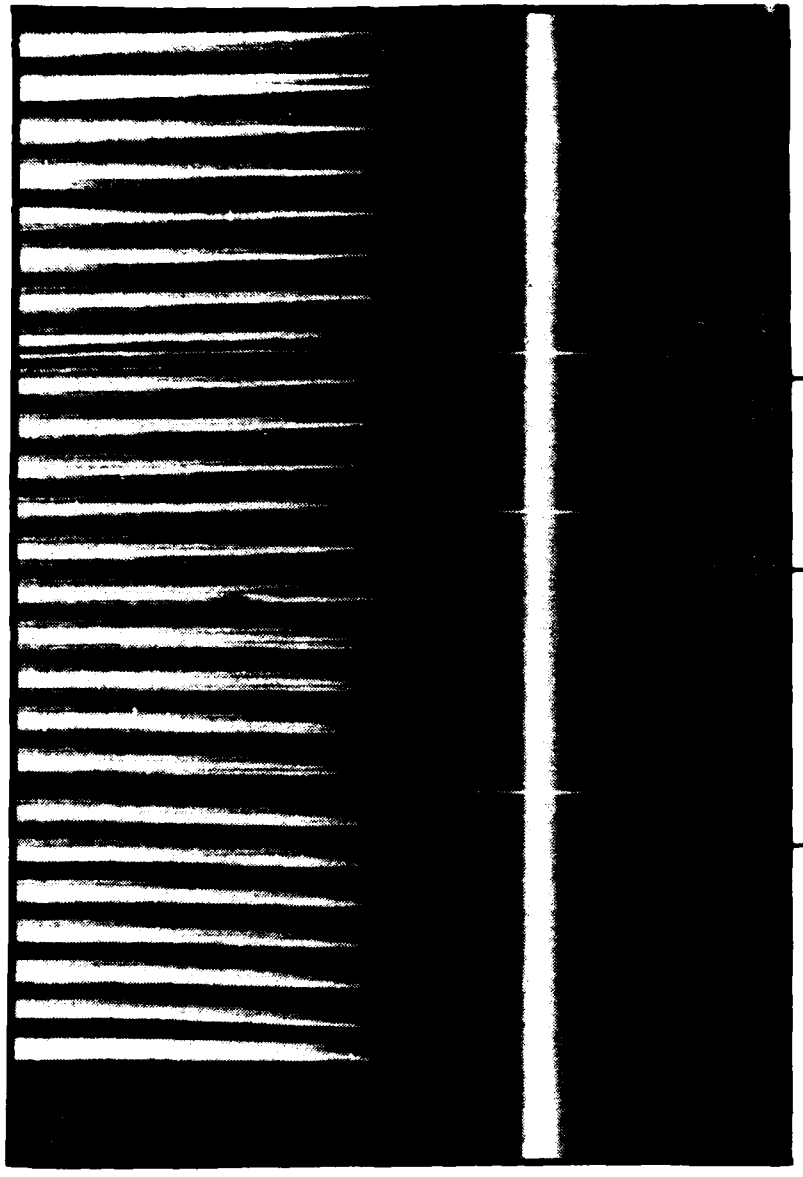

Figure 3.1-29 Flaw annotated DR of battery #109

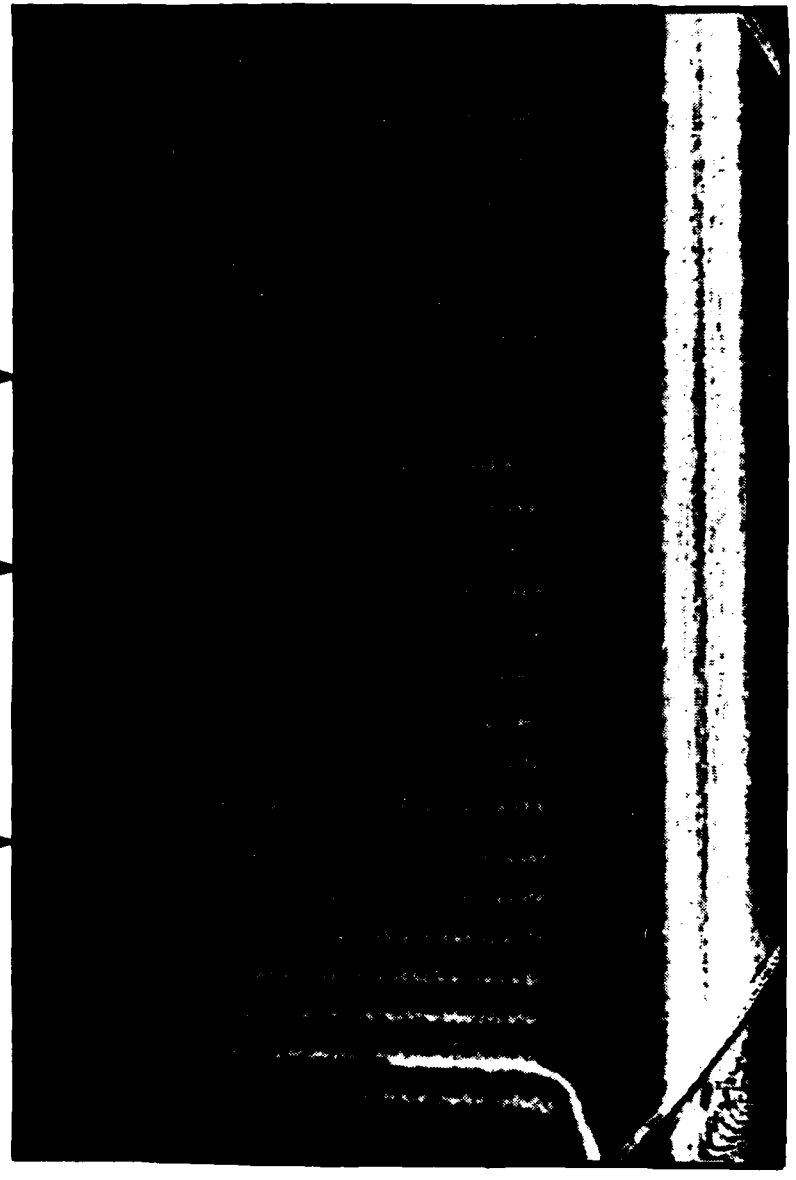

Figure 3.1-30 CT view of battery #109

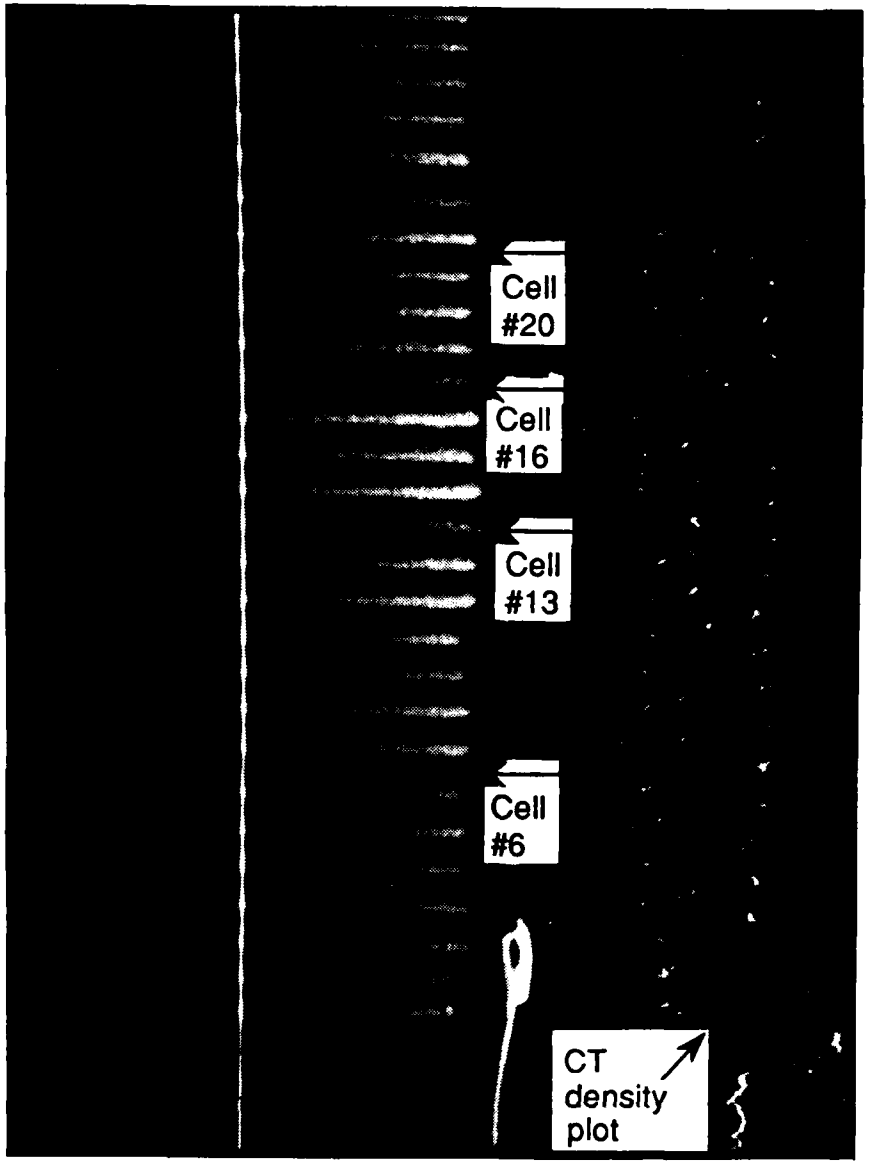

Figure 3.1-31 Ct view and density plot of anomalous cells in battery #109

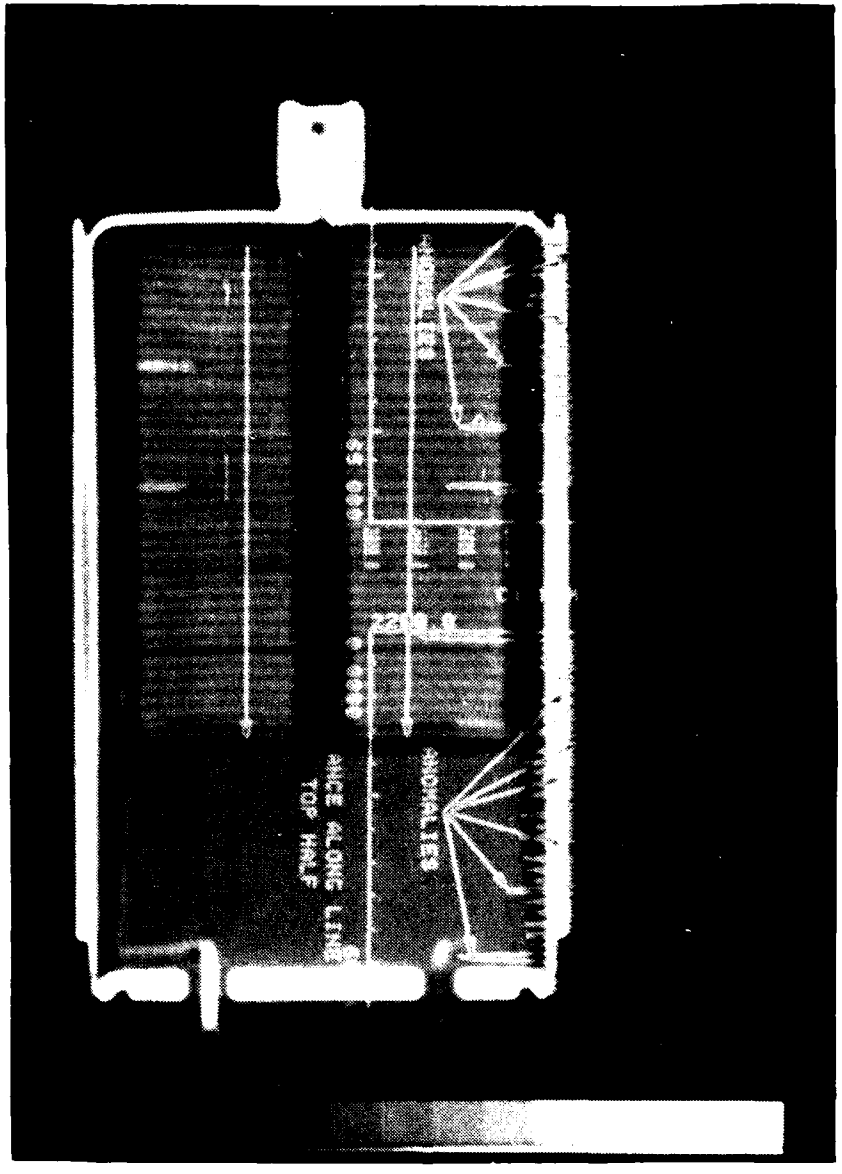

Figure 3.1-32 Ct view and density plot of defective cells in battery #109

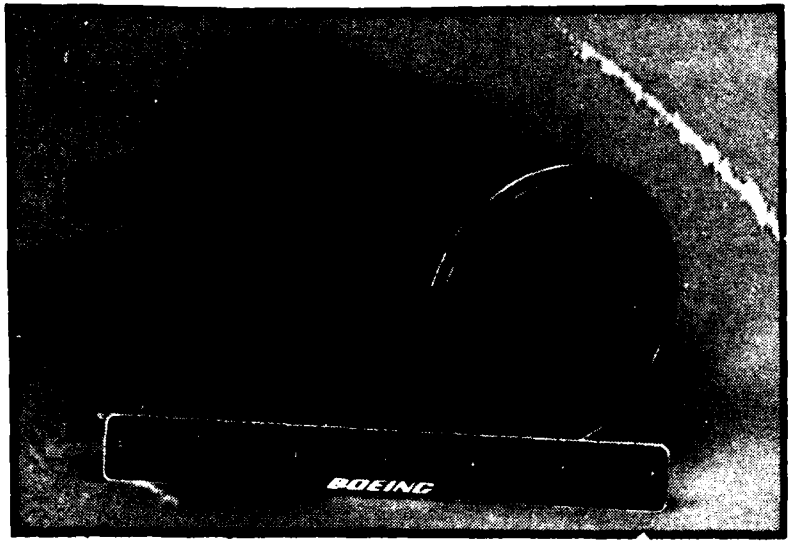

Figure 3.1-33 Fired battery #112

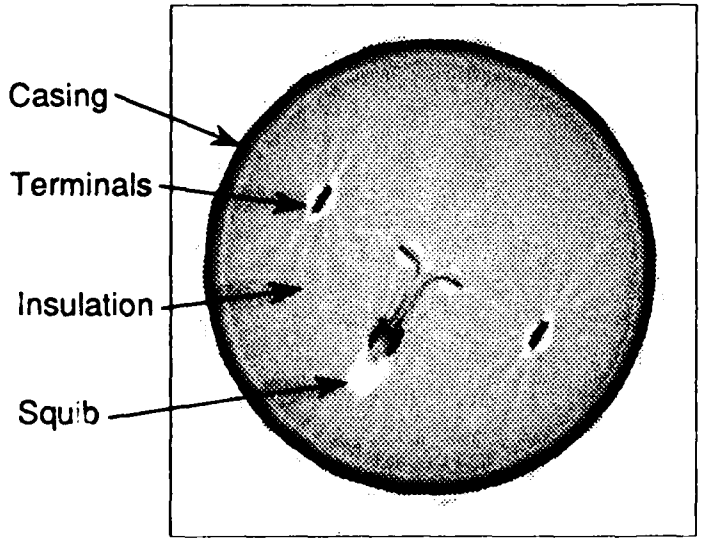

Figure 3.1-35 CT view of spent squib in battery #112

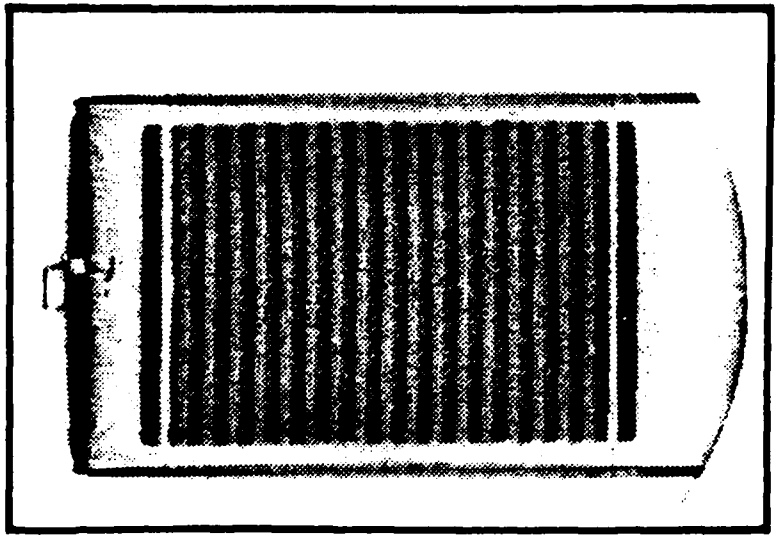

Figure 3.1-34 CT view of unfired battery #111

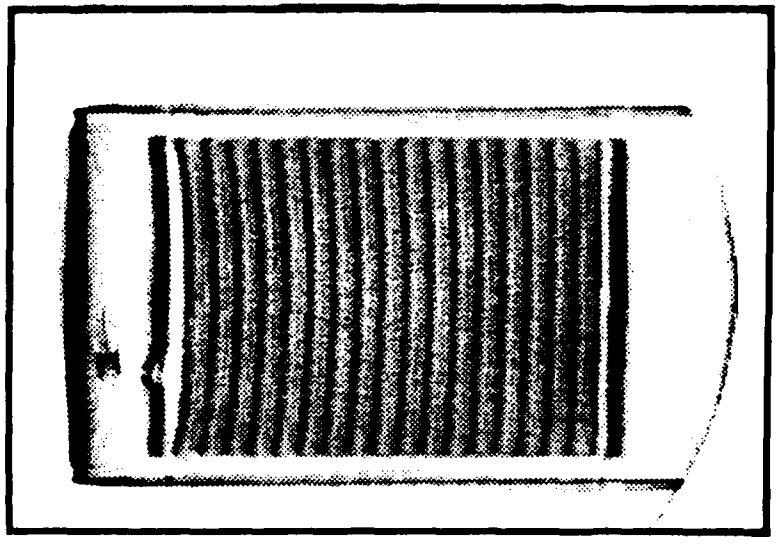

Figure 3.1-36 CT view of cell slump in fired battery #112

accurate calculation of Compton and photoelectric energies. The Compton image is directly related to electron density while the photoelectric image is related to density and atomic number.

The dual energy imaging was applied to the two identical batteries, one fired (#112) and one unfired (#111). Figures 3.1-37 and 3.1-38 are the unfired battery Compton and photoelectric images respectively. Figures 3.1-39 and 3.1-40 are Compton and photoelectric images, respectively, for the fired battery. The results show somewhat greater image definition in the manipulated and combined images than in either single energy image alone. The standard CT image is similar to the Compton image, which is considerably different from the photoelectric image. In the analysis of failed batteries, one would look for localized "clumping" of specific elements (e.g., Fe) which indicates shorting. The photoelectric image provides a method to locate the elemental variation in the battery. The image in Figure 3.1-40 is of a successfully fired battery, showing the typical cooling pattern and mixing of the elements. The dual energy process would be of advantage in the analysis of fired batteries that did not perform successfully.

Battery #115 was another fired battery used on a SRAM missile. This battery had considerably altered external features caused by the heat of firing on the adjacent material. The battery CT image is included in the Figure 3.1-21 multiple battery CT view. Individual cells are resolved and show density variations; some slumping or waviness can be seen upon close inspection.

3.2 Category 2 - Safe and Arm Devices

3.2.1 Hardware Description

The IUS Safe and Arm (S&A) Device, PID# 020201, was added to the closed systems task when it was learned that potentially catastrophic failures had occurred on assigned space missions with this item. The S&A device is generic to small solid rocket motor (SRM) applications and are "one shot" devices. An expended IUS S&A is pictured in Figure 3.2-1. The S&A device is an integral sealed electromechanical part with a motor/rotor assembly. When the S&A is commanded "ARM", the rotor is energized and rotates the detonator cord parts into position. A subsequent "FIRE" command sets off the firing train (detonator, cord, ignitor) of the SRM. There have been acceptance test failures of the S&A where the rotor failed to fully rotate when commanded. These test failures were attributed to contamination (contamination may be in many forms, e.g., dust, plastic, sealent material, rust, metal particles, etc.) within the motor/rotor gap. This gap varies between 0.13 to 0.38 mm (0.005 to 0.015 in) and nominally runs 0.18 to 0.36 mm (0.007 to 0.014 in).

3.2.2 Inspection Goals

The CT goals were to: 1) inspect the sealed device and to image debris as small as 0.05 to 0.13 mm (0.002 to 0.005 in) in diameter, 2) inspect the rotor gap for uniform clearance and evidence of contamination, and 3) inspect other electrical and mechanical components of the device.

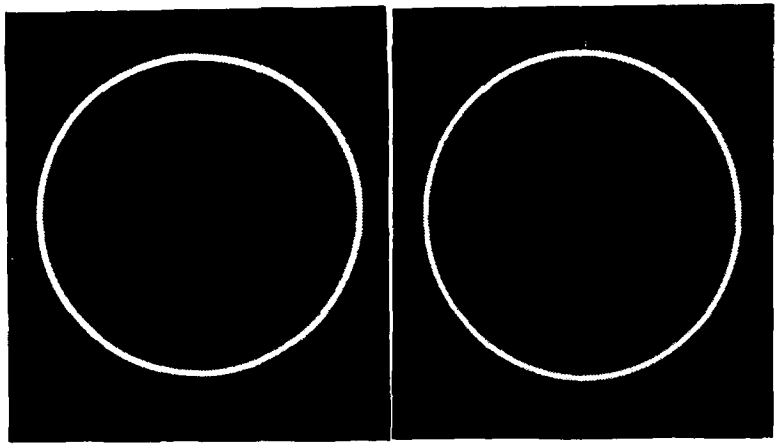

Figure 3.1-37 Dual energy Compton image of unfired battery #111

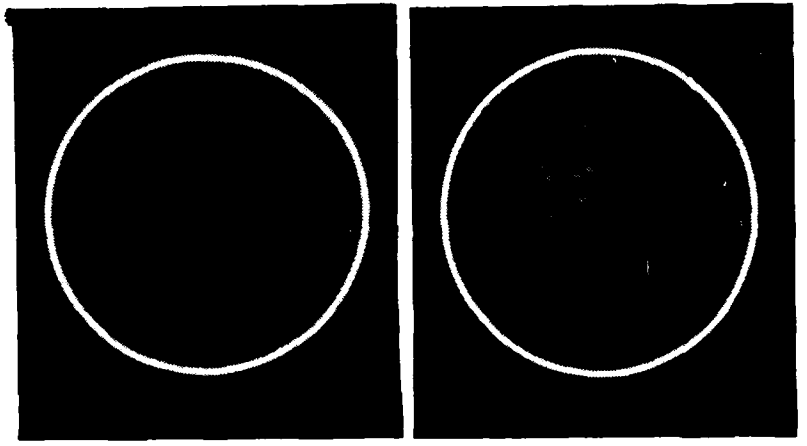

Figure 3.1-38 Dual energy photoelectric image of unfired battery #111

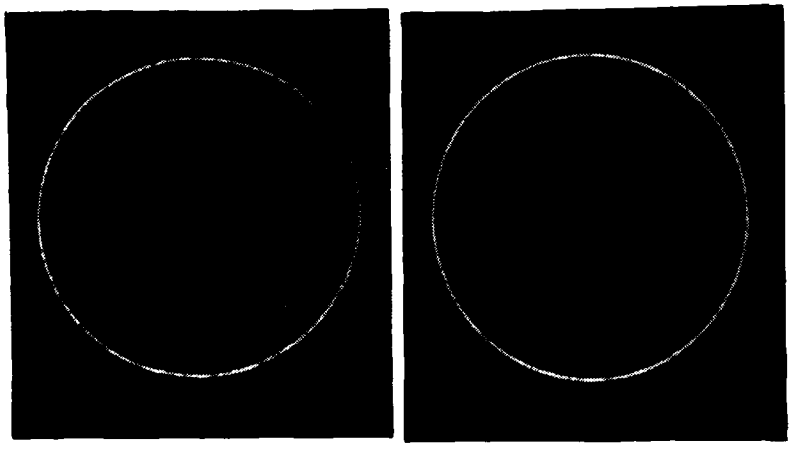

Figure 3.1-39 Dual energy Compton image of fired battery #112

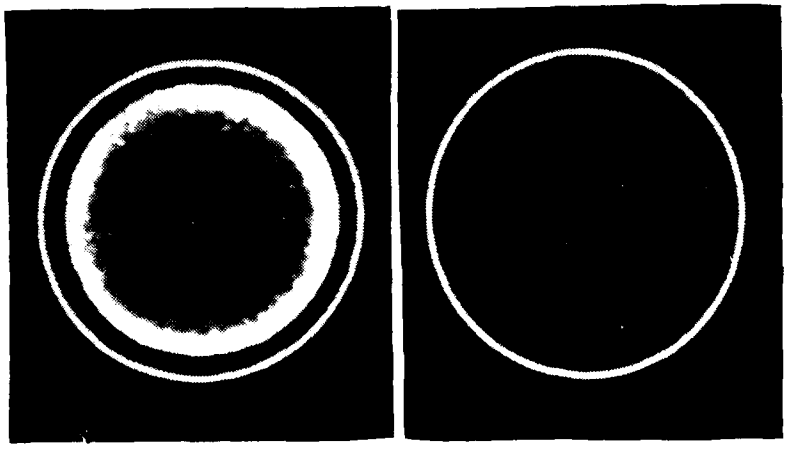

Figure 3.1-40 Dual energy photoelectric image of fired battery #112

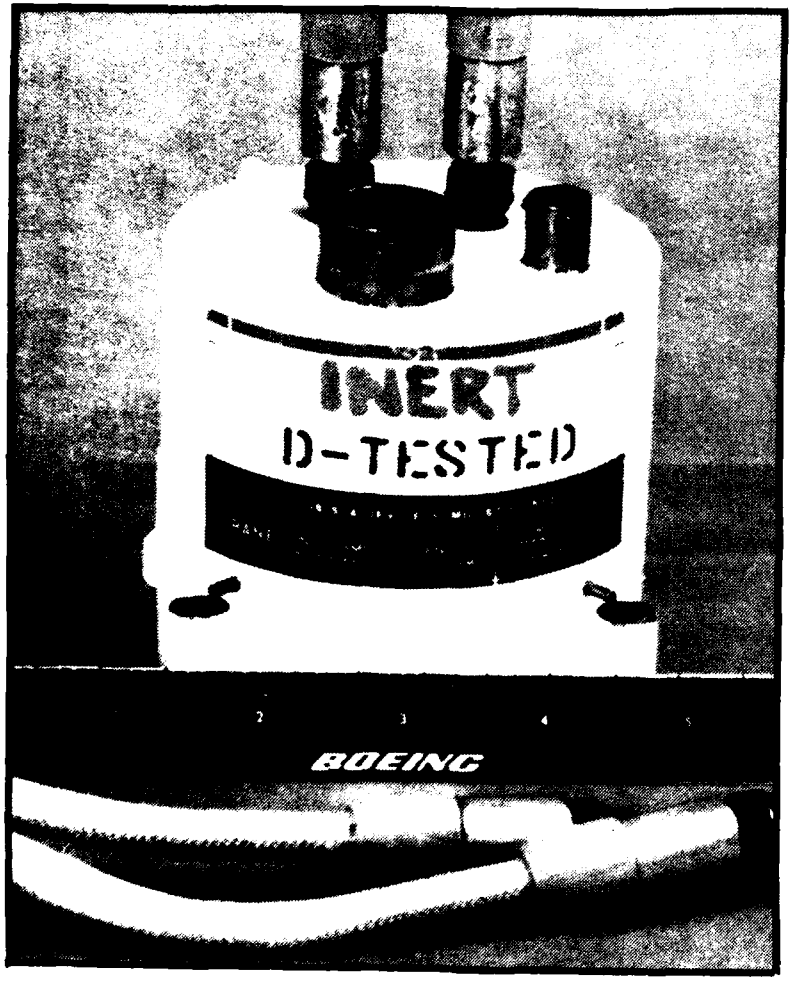

Figure 3.2-1 Safe and Arm (S&A) device

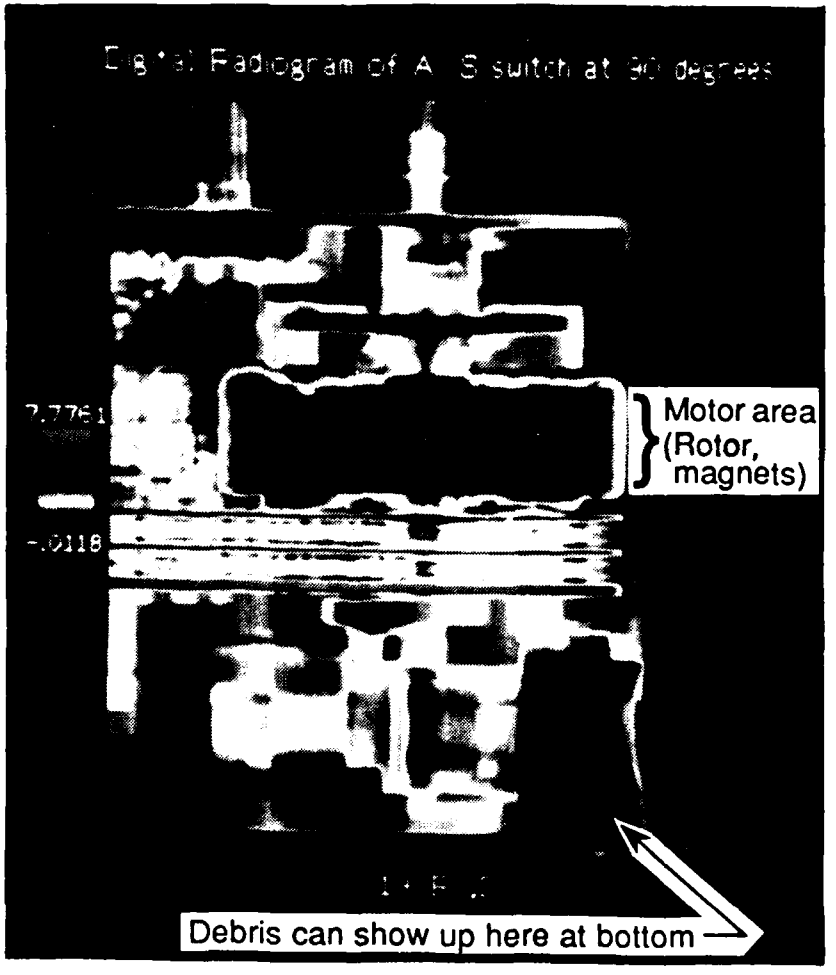

Figure 3.2-2 DR of S&A device

3.2.3 Results

An expended (fired) S&A device was inspected on System B. The results were of high interest to IUS engineering and met all test objectives. A digital radiograph, Figure 3.2-2, was first taken to establish CT slice heights. The motor gap, windings, and broken magnets were clearly visible in a CT slice, Figure 3.2-3, taken 58 mm (2.28 in) from the bottom of the S&A. A slice taken 5.1 mm (0.20 in) from the bottom, Figure 3.2-4, revealed debris from the firing that had settled to the bottom of the device. Any debris at all amounts to intolerable contamination in an unfired unit. The visible debris shown in Figure 3.2-4 varied in size from 2 mm (0.080 in) down to less than 0.15 mm (0.006 in).

3.3 Category 3 - Command Signal Decoder

3.3.1 Hardware Description

The Command Signal Decoder (CSD), PID# 020203, pictured in Figure 3.3-1 with the aluminum cover removed, is an example of an intricate mechanical device that could potentially benefit from CT examination. The CSD is used to inhibit unauthorized launch of ICBM (Minuteman and Peacekeeper) missiles by virtue of a 24-bit code. The code is mechanically determined by the positions of 24 steel pins with flats surrounding a rotary sprocket. The positions of the pins, both in and out, as well as rotation angle, determine the status of the coding. Although the CSD is primarily mechanical in operation, missile firing currents do pass through it.

CSD units in the field may need to be opened when a mechanical fault is experienced during periodic system test and code verification. This requires removing the CSD from the missile system and a handcarry, under guard, back to a distant repair facility for authorized entry and repair. This operation is very expensive and time consuming.

3.3.2 Inspection Goals

A sprocket buried inside the unit must turn to unsafe the system. The sprocket will only turn if all pins are aligned so that their flats face inward toward the center. The width of the flats is less than 1 mm (0.039 in) wide on the steel pins. The primary CT inspection goal for this device was to image the pin configuration sufficiently to determine the condition of the system. Other mechanical and electrical configurations were also of interest.

3.3.3 Test Conduct and Results

The CSD unit was scanned on three CT systems: B, F, and I. All three systems successfully imaged the flats on the pins, and thus the code. The pin flats and the cover box outline are clearly visible in the System F image, Figure 3.3-2. CT views at other slice planes showed reasonably good detail to determine configuration and clearances of various components.

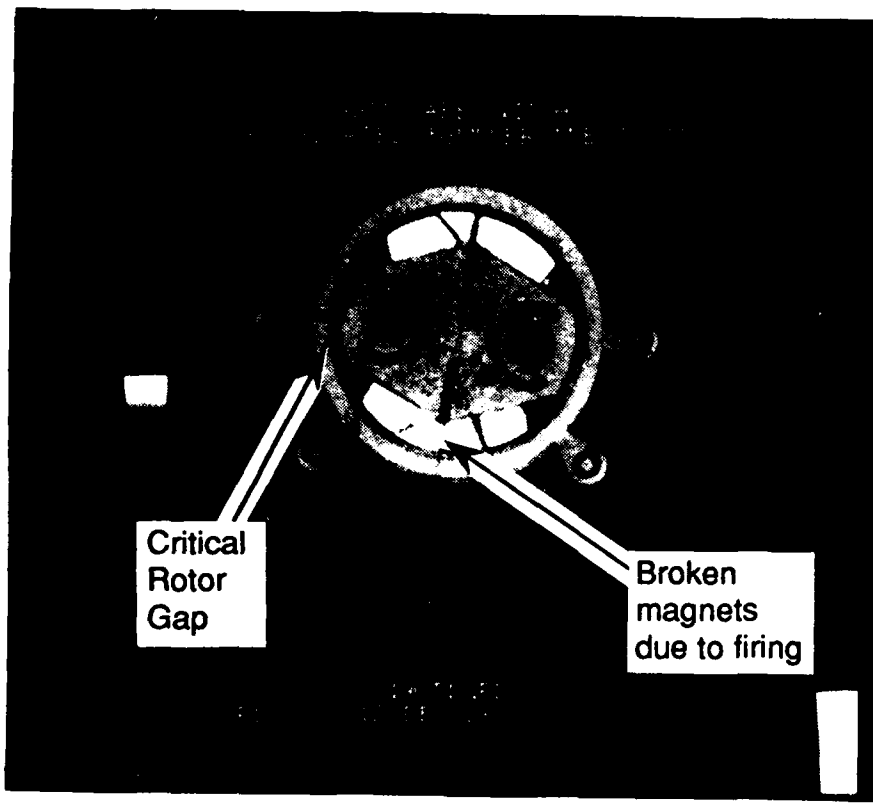

Figure 3.2-3 CT view of S&A device rotor gap and broken magnets

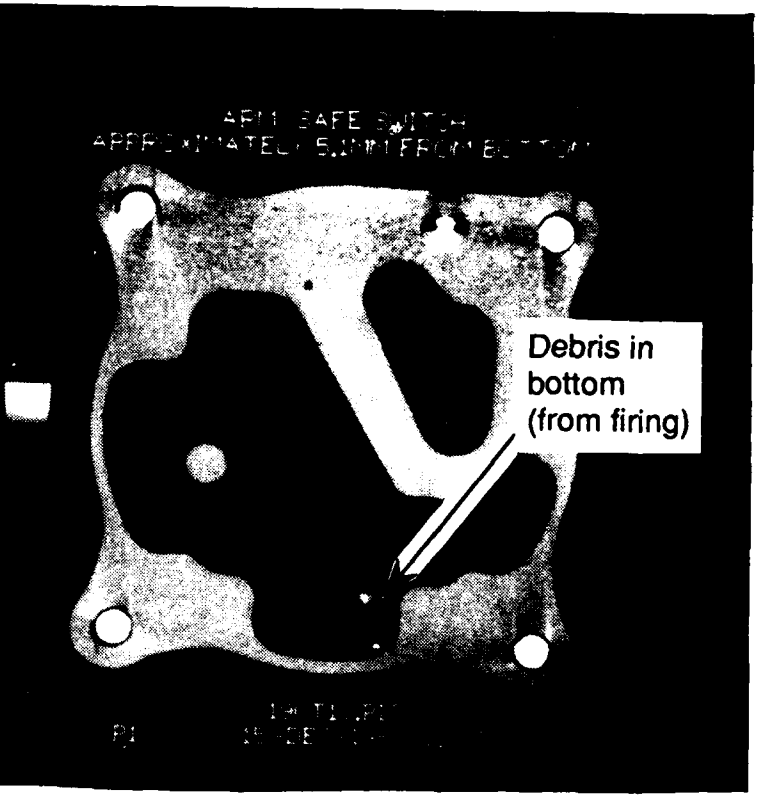

Figure 3.2-4 CT view of debris at bottom of fired S&A device

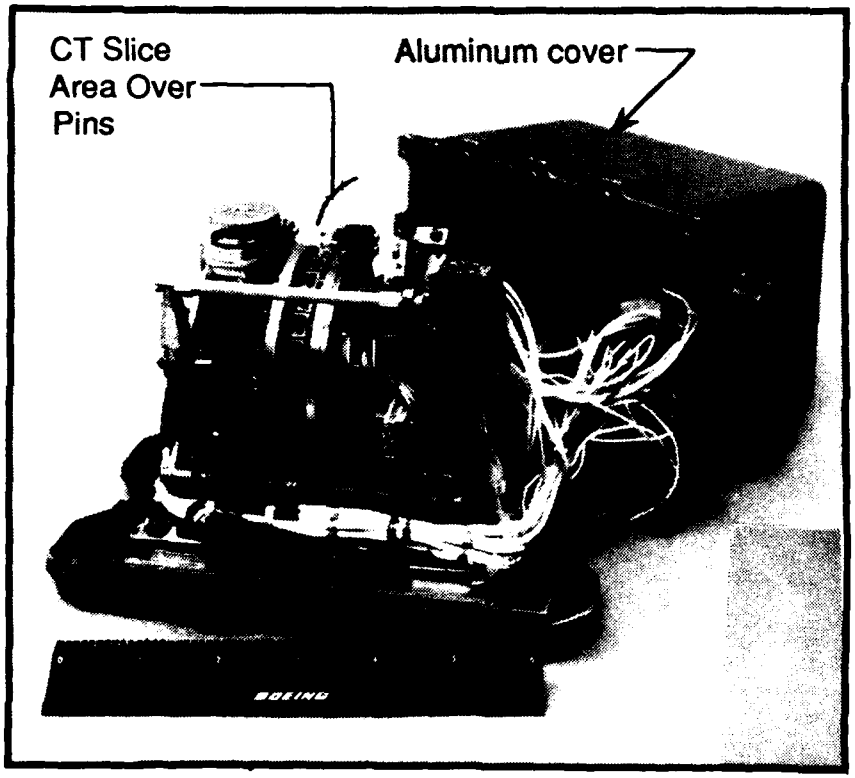

Figure 3.3-1 Command signal decoder (CSD)

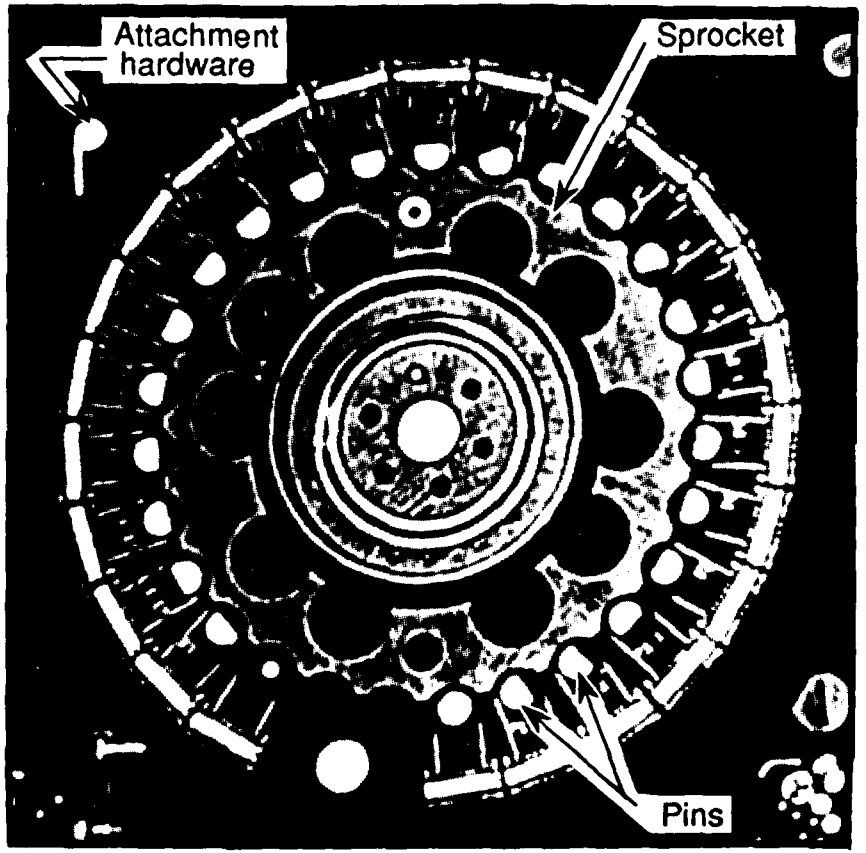

Figure 3.3-2 CT view of CSD showing pin configuration

3.4 Category 4 - Aircraft Gear Drive Assembly

3.4.1 Hardware Description

A steel differential gear drive assembly, used for the 747 stabilizer jackscrew, was obtained from the commercial airplane division of Boeing. The jackscrew has internal features not readily discernable with other NDE techniques. Differential gears, for example, represent a complex assembly requiring precise alignments. An assembly specimen, built for CT testing, is pictured in Figure 3.4-1 (note: the assembly is normally installed in a protective metal housing). The steel gear drive specimen is mounted on an acrylic stand, which is stable in both the horizontal and vertical position. The weight is approximately 6.8 kg (15 lbs) and the size is 25 cm by 15 cm by 15 cm (9.8 in by 5.9 in by 5.9 in).

3.4.2 Inspection Goals

The testing goals were to image and spatially define the components of the gear assembly, the bearing, and the shim clearances. Under load, the bevel gears must mesh correctly for proper operation of the gear. Any indications in the CT image that could assess the quality of the alignment and meshing surface configuration were of interest. Heavy beam attenuation in the steel body was considered a serious limiting factor.

3.4.3 Test Conduct and Results

The gears were successfully scanned on both System H and System I. A full volumetric set of images were obtained on System H at 2 MeV. The data demonstrates the usefulness of CT in observing the gear interface gaps, the shims, and bearing components. Both Systems H and I imaged the entire gear train through the main drive shaft, which is more than 25.4 cm (10 in) in length. A DR image is shown in Figure 3.4-2 and, much like film radiography, provides little information about the assembly. A CT slice image, taken through the length of the drive shaft, is shown in Figure 3.4-3. The lengthwise CT image was surprisingly clear and demonstrates the penetration ability of a 2 MeV system into steel objects.

Figure 3.4-4 is a 3 mm (0.12 in) thick CT slice taken normal to the axis showing gear teeth and bearing. A steel bolt holding the gears together appears as the off-center circle in the middle of the picture.

A series of contiguous axial CT slices, 3 mm (0.12 in) thick, were taken over the length of the gear assembly on System H. These data slices were later processed and displayed on the Boeing PIXAR imaging system. A solid appearing image of the gears with "peelable" layers from all three orthogonal surfaces was produced, providing a highly effective examination technique for the gear assembly. An even more effective analysis method will be possible when 3D isometric viewing capability is installed on the system.

The results of the CT scans verifies the penetration and imaging ability of the high-energy CT systems on thick, heavy aircraft and aerospace parts. Both H and I CT systems have resolution capability in the 0.5 to 1 lp/mm (1 to .5 mm resolution) range.

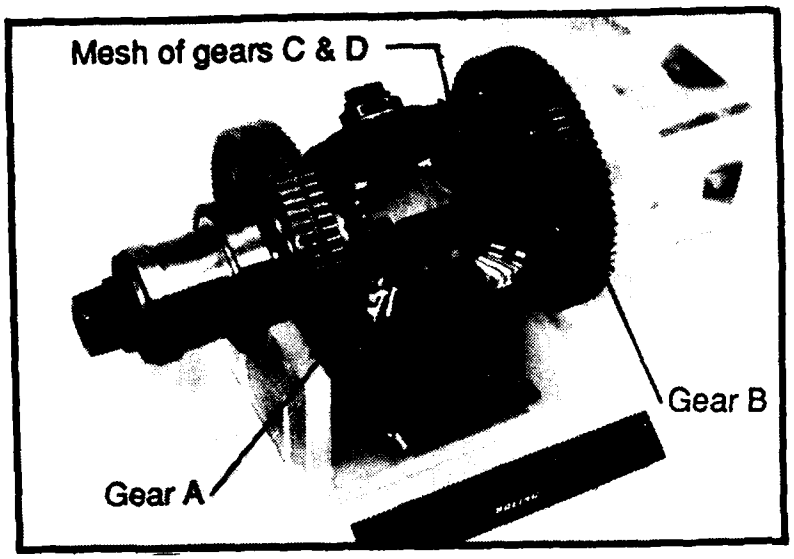

Figure 3.4-1 Aircraft gear drive assembly

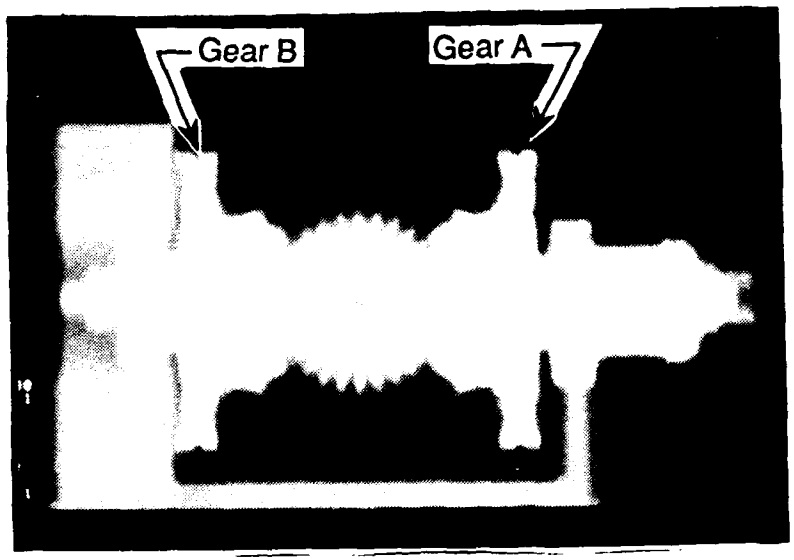

Figure 3.4-2 DR of aircraft gear drive assembly

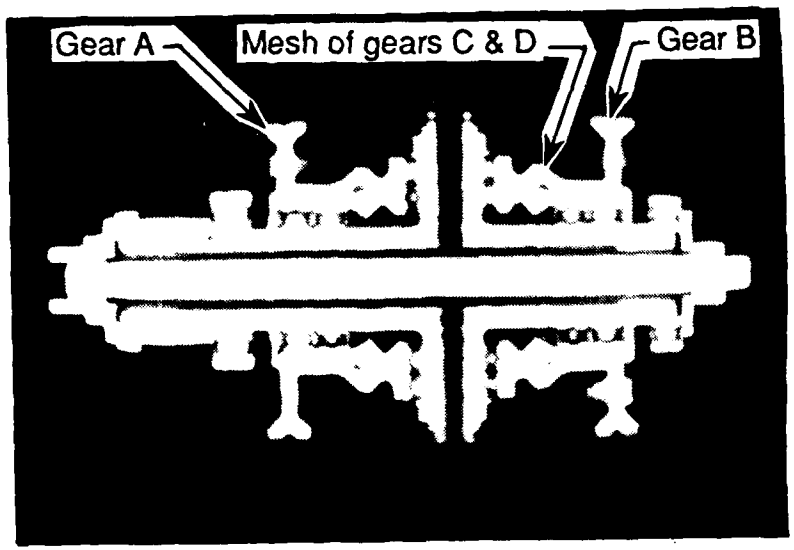

Figure 3.4-3 2 MeV longitudinal view of gear drive assembly

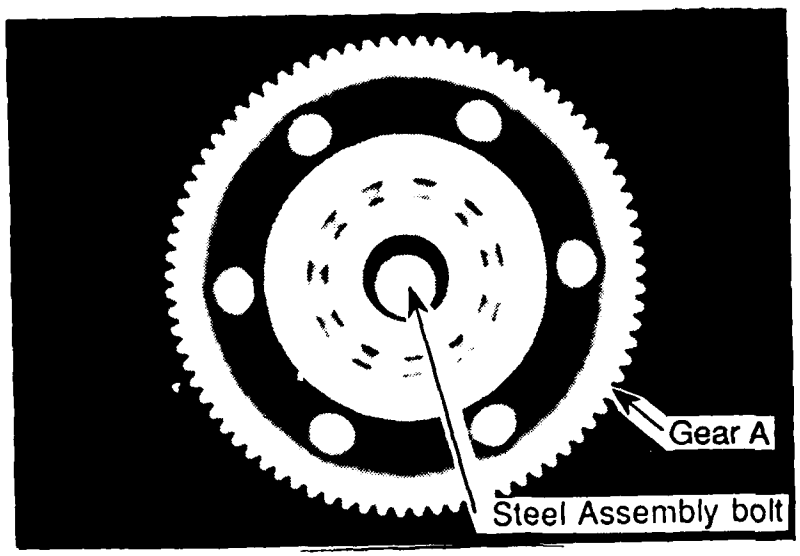

Figure 3.4-4 Axial CT view showing drive gear, bearing and off-center assembly bolt

Although desirable, actual shim and bearing clearance measurements of less than 0.5 cm (0.020 in) were not possible.

3.5 Category 5 - Aircraft Hydraulic Slat Actuator

3.5.1 Hardware Description

A hydraulic actuator for the leading edge slat in a Boeing 737 wing, shown in Figure 3.5-1, was selected as a potential closed systems candidate. The actuator dimensions are 15 cm (5.9 in) maximum cross section and 30 cm (11.8 in) long. The actuator has an anodized aluminum body and a steel piston assembly.

3.5.2 Inspection Goals

The major challenge was to penetrate the heavy steel and aluminum structure and to image the many internal steel parts and 'O' rings. Primary interest was with details in the multiple-step latching mechanism in the center of the unit.

3.5.3 Test Conduct and Results

System I was used to provide two longitudinal slices: one vertical and one horizontal. The lengthwise CT slice was highly effective in imaging the internal parts of the actuator. The 1024 x 1024 image of the actuator was obtained in under 5 minutes including scan and reconstruction time. Figure 3.5-2 is a standard 5 mm (0.2 in) thick longitudinal slice through the part and appears fairly sharp. However, zoom reconstruction images of the latching mechanism near the actuator center appear fuzzy. The actuator was subsequently sent to the smaller format System B to obtain greater resolution. A 1.5 cm (0.59 in), 20 slice (1 mm (0.04 in) width at 0.75 mm (0.03 in) spacing) series near the middle of the actuator, was taken on System B. At the time, System B had a cobalt-60 source installed. The cobalt-60 source did not provide the expected, typically higher, resolution offered by System B. This was due, in part, to the unexpectedly low intensity (13 Curie) cobalt source with a relatively large 3 mm (0.12 in) spot size.

A section reconstruction, or synthetic tomogram, was constructed along the center line of the axis from a series of 20 contiguous axial CT slices taken through the actuator near the middle. The top and bottom axial slices and the resulting synthetic tomogram image are shown in Figure 3.5-3. The image is not sharp, however, it meets the minimum resolution requirements of the actuator design group. Higher resolution images could have been obtained, it was discovered in a test performed later, using the reinstalled 420 kVp source instead of the low-intensity cobalt-60 source. Two axial CT views, one taken with the cobalt-60 source and one taken with a 420 kVp source, were obtained and are shown in Figure 3.5-4. The 420 kVp image is shown as the clearer image on the right.

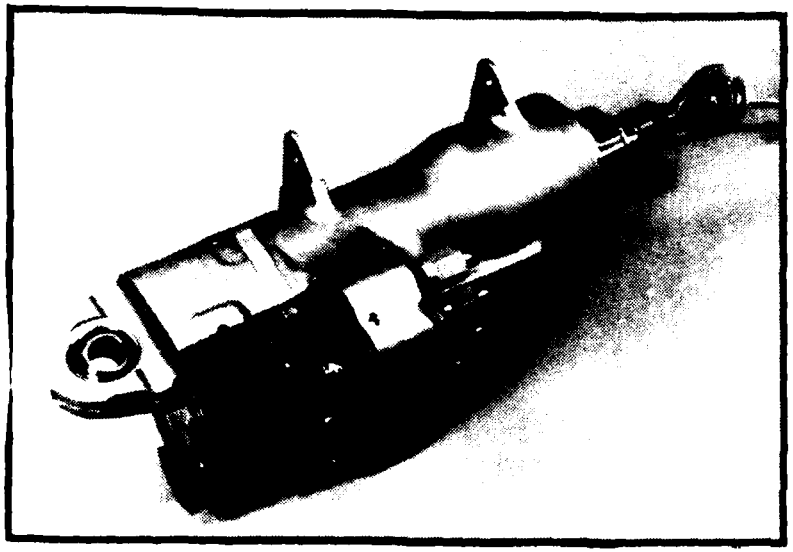

Figure 3.5-1 Aircraft hydraulic slat actuator

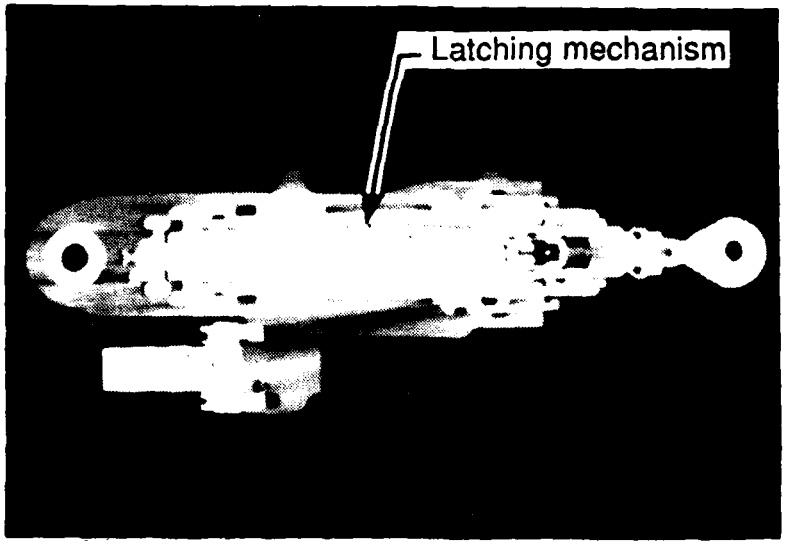

Figure 3.5-2 Longitudinal CT view of hydraulic slat actuator

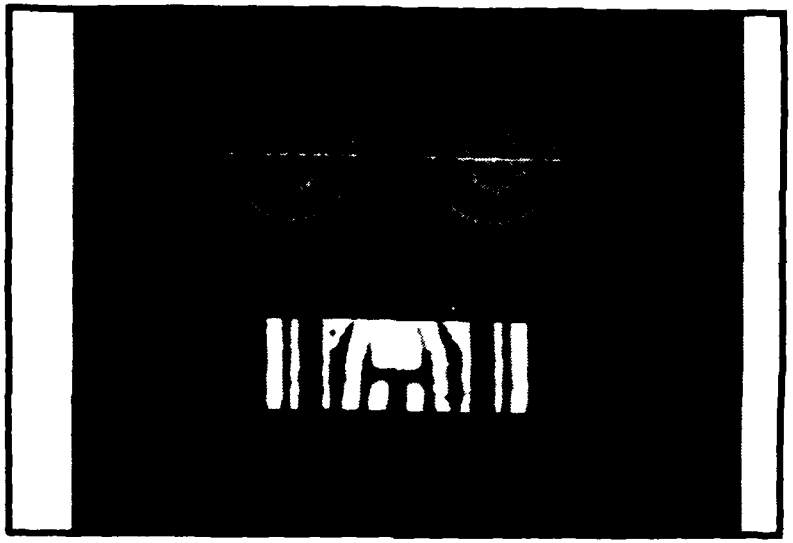

Figure 3.5-3 Synthetic tomographic view (longitudinal) of actuator

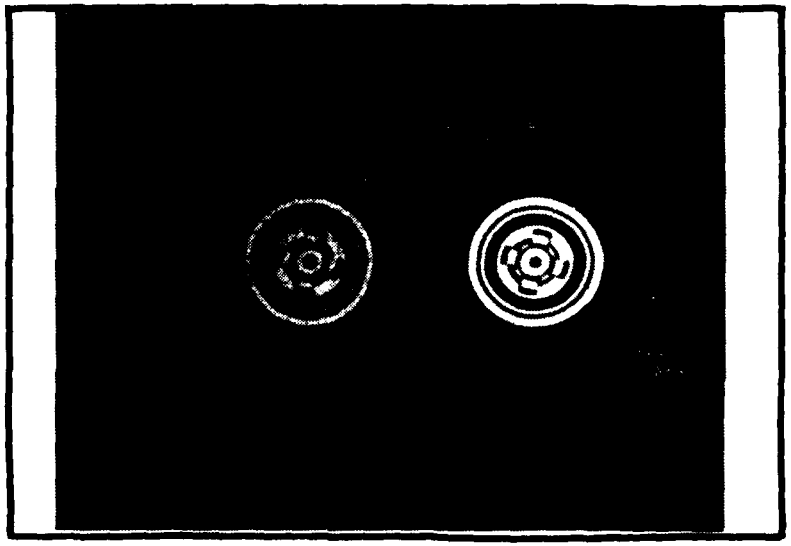

Figure 3.5-4 Two axial CT views of the actuator using cobalt 60 and 420 kVp sources

4.0 COST BENEFIT ANALYSIS

A primary objective of the CTAD program is to assess what economic benefits are obtained from CT scanning a component. It must be pointed out that economic benefits can be realized in more ways than by producing a less expensive component or by having a less expensive inspection method. Economic benefit can also be realized from increased component performance and higher component reliability (especially for mission critical components). CT has the potential to provide the quantitative inspection information necessary to assist engineering design and manufacturing quality control. Areas that could have potential payback for CT inspection are identified in this study: production inspection, prototype development and failure analysis. Production inspection economic payback is in the area of large-volume and/or high-value items that utilize inadequate or high-cost inspection methods. Prototype development and failure analysis inspections are low volume. The economic payback for prototype development would come from being able to examine a "closed system" component in final configuration, prior to full-scale production. This would allow verification of engineering design and component functionality, and evaluation of potential failure mechanisms. The economic payback for failure analysis inspections would come from evaluating failure mechanisms in mission critical components. This "first look" at economic payback examined during this preliminary testing task is based on purchasing CT scan time and the usefulness, or relevance, of the data obtained.

4.1 Thermal Batteries

The cost of the thermal batteries varies from $100 to $4000, as is shown in Figure 3.1-1. The cost is directly dependent upon production rates and difficulty of construction. During production phases of a given design the typical production rate is in the range of from 300 to 2000 batteries per month. The criticality of each battery is listed in column 4 of Figure 3.1-1. All have at least a mission essential rating. Only battery #108 and #110 are listed as having top criticality (A). They are used on ALCM and re-entry vehicle assignments, both of which constitute mission strategic importance.

Current NDE inspection techniques for thermal batteries are electrical testing, film radiography, leak testing and dimensional measurements. Film radiography costs, excluding evaluation costs, are nominally estimated at $3 to $15 per battery. This compares to a CT cost-per-slice range of $8 to $65, as subcontracted under this program, estimated from hourly rates but not including setup and analysis time. If a DR alone proved to be sufficient, the scan cost could be as little as $5 (based on a less than 1 minute scan). This would be competitive to present conventional methods and could provide more detail.

Figure 4.1-1 shows a cost analysis of purchasing a $1.5M CT system and amortizing the purchase over 5 years. At a $450,765/year machine cost and assuming 2000 hours/year operation at a labor cost of $45/hour, the cost/hour is about $270. A breakeven $5/battery inspection rate would be about 54 batteries/hour. While this production rate is possible, assuming DR's are used primarily and multiple batteries can be mounted at one time (batch inspection), it is probably at the limit of the technology. With this simple economic analysis, CT appears to be of marginal

economic benefit. CT machine costs will need to be reduced significantly if a benefit, based solely on meeting current inspection needs, is to be realized.

Machine Cost	$ 500,000	$1,000,000	$1,500,000
Cost of Money (@ 7%)	$ 201,276	$ 402,552	$ 603,826
Maintenance @ $30K/yr	$ 150,000	$ 150,000	$ 150,000
Total Cost	$ 851,276	$1,552,552	$2,253,826
Cost/Year (5 years)	$ 170,255	$ 310,510	$ 450,765
Hourly cost (2000 hours/year)	$ 85/yr	$ 155/hr	$ 225/hr
Cost Plus Inspector	$ 130/hr	$ 200/hr	$ 270/hr
Throughput for $5/Battery Inspection	26/hr 52,000/yr	40/hr 80,000/yr	54/hr 108,000/yr

Figure 4.1-1 Estimate of battery throughput for implementation of CT

The cost analysis will change significantly if requirements for higher quality and consistency in production, resulting in a higher rejection rate (currently 1 to 5 percent), are specified by the customer. For example, CT showed the ability to perform automated cell counting, detect cracks in cells, cracks in insulation and imaging of screen meshes which conventional inspections cannot perform to date. A higher rejection rate at the production level should result in fewer failed batteries during sample lot testing and a higher reliability rating.

In the area of failed batteries, CT may provide an important evaluation tool. Battery manufacturing lots are qualified by test firings. If batteries fail during testing (currently about 0.1 percent of the time), then the cause of failure must be resolved to everyone's satisfaction, or the lot may be rejected and/or reworked at considerable economic impact with consequential damaging impact to major program schedules. CT (both conventional and dual energy) could provide important failure analysis information under these circumstances and could be cost effective at the commercial testing rates.

4.2 Safe and Arm Devices

The cost of a S&A device of the type tested, is in the $30K to $40K range, depending on the quantity procured. A Boeing two stage IUS System uses four to six of these

devices depending on the launch vehicle used for the mission: two devices are used for each of the two solid rocket motors (SRM's), one serving as backup, providing redundancy for SRM ignition. The unit itself has two detonating cords, either of which will ignite the SRM. However, if the internal rotor fails to properly align the detonators with the ports, neither detonating cord is initiated, resulting in failure of the S&A to ignite the SRM. SRM ignition is then accomplished by the redundant S&A device. The significance of a failure of either rocket motor to fire is catastrophic. Potentially, a $300 million satellite could be lost.

The type of CT images shown in Figures 3.2-3 and 3.2-4 can provide usable accept/reject criteria for quality assurance. Due to the suspected contamination failures of the device, contamination control facilities and procedures have been implemented for future production. CT image data, obtained at an estimated cost of $500 to $1000 per unit, has been requested for a future device to determine the effectiveness of the contamination control measures implemented. This will eliminate the need to sacrifice a device to Destructive Physical Analysis (DPA), which is costly, in order to evaluate the effectiveness of the contamination control corrective action. There is no radiographic inspection technique that is currently being used.

4.3 Command Signal Decoder

The Command Signal Decoder device is worth approximately $200K. The device is not currently in production, but a large number are still in service. However, there is little economic incentive to use CT for this particular device since the unit must be opened if there is a failure. The Command Signal Decoder was evaluated, as an example, to demonstrate the potential of utilizing CT to inspect similar closed systems.

4.4 Aircraft Gear Drive Assembly

The 747 gear drive assembly is a difficult mechanism to assemble. Gear clearances are critical for smooth, noise-free operation. A way of determining a successful assembly, outside of actually operating the gear under load, does not currently exist. When first assembled, the gears are checked for tooth contact and backlash. Out of tolerance bearing, shims, etc. create a high rework rate during manufacturing and assembly. Disassembly and rework are required 99 percent of the time. Rework consists primarily of shim modification and is repeated on the average of 4 times before the unit is acceptable.

The cost of the gears is approximately $25K. The possibility of failure in service exists, but is not significant. The design of this particular unit involves redundant load bearing capability because loss of the jackscrew due to gearbox failure could be quite serious in the performance of the aircraft, particularly when critical flight surface control malfunction. No failures have occurred. The gear drive assembly has a C category rating or average cost and high reliability requirement.

The advantage of CT inspection to assure correct assembly has not been established. The precision required to provide an obvious economic incentive to use CT was not obtained. CT may be advantageous in some development studies.

4.5 Aircraft Hydraulic Slat Actuator

The cost of the actuator is approximately $10,000. Because of the complicated assembly process, an assembled unit requires an understanding of the many parts and pieces contained inside the actuator. High-resolution (2 to 4 lp/mm) CT may be able to provide the necessary resolution while medium resolution (0.5 to 2 lp/mm) cannot. CT could be very helpful during the design and check out of each manufactured prototype actuator. Once the design phase is completed, however, the emphasis on inspection is much less. Whenever failures occur however, CT is beneficial to observe the internal part configuration before the parts are altered in position during disassembly.

5.0 CONCLUSIONS AND RECOMMENDATIONS

Generally, CT provides informative data on the internal configuration of closed systems beyond that provided by conventional film radiography. A particular usefulness of CT in closed systems is in engineering evaluation of the assembly during prototyping or failure analysis. CT provides highly detailed information on a thin slice through a complex System. With the use of multiple CT slices and synthetic tomographic reconstruction, high-resolution images can be obtained along selected planes. High-resolution digital radiography compares favorably to film radiography in terms of speed and exceeds film radiography in ability to resolve individual cell details.

5.1 Thermal Batteries

Medium resolution (0.5 to 2 lp/mm) CT and DR are marginally equivalent to radiography in terms of cell layer structure resolution, but they do not have the parallax problem of the film technique. High-resolution (2 to 4 lp/mm) CT systems have DR's that compete very well with film for resolution; the dynamic range, however, is superior.

DR and longitudinal CT slices are better than axial CT slices for quick-look cell structure layout and squib/primer information. A single longitudinal CT slice can provide desired information concerning lead runs and connections if the appropriate slice location is chosen, i.e., through diametrically opposite terminal and lead sets.

The axial CT slices provide more information than is currently desired by the manufacturer for standard quality control inspections. In fact, defects such as cracked material layers in cells and insulation were found that were unknown to the manufacturer. Axial slices are effective when conducting detailed study of layers within cells and specific dimensional information, such as squib and heat paper configuration. Many axial slices (4-6 per cell) are required to map the battery entirely.

Multiple battery (batch) inspection is possible with CT to improve the economics. Considerations are: 1) the mounting of the batteries to assure proper slice location and 2) possible loss of resolution with more mass intercepting the X-ray beam. CT and DR offer some significant image processing advantages for automated inspection, as shown by the ability to count cells and detect defective cells. A single CT slice through multiple batteries (four to six) could provide, as a minimum, cell count and cell orientation information.

Failed batteries, resulting primarily from lot acceptance testing, can be inspected with CT to assist the important analysis task. Currently, the only alternative to film radiography in failure analysis is dissection, which is highly detrimental to the analysis. Economic incentives exist for understanding the failure mechanisms of thermal batteries since they are used predominantly in systems (missiles, rockets, pilot ejection seats) where failure of the mission could have a serious economic impact.

5.2 Other Closed Systems

CT inspection of various mechanical and electromechanical closed systems, have resulted in images suitable for engineering evaluation of the assembly quality. Engineering analysis data and failure analysis studies are the most obvious applications.

CT inspection of S&A devices may have great benefit to IUS engineering in the areas of failure analysis and contamination control. In addition, select CT slice locations also can provide highly detailed and valuable information about the as-constructed part. The inspection process would be continued through post-manufacturing and pre-installation. The inspection would screen undesirable or rejectionable sealed units for physical integrity and contamination.

It would be impractical and economically unsound to purchase a CT for just S&A device production inspection. Expected usage rate of this device is sixteen per year for the next three years. CT facility rental, however, for production and developmental inspection is practical. CT has been requested for evaluation of a lot sample of the current build of S&A devices for effectiveness of contamination control corrective action. CT has been suggested for use as a failure analysis tool for S&A's that may fail pre-installation acceptance testing. This would eliminate the need to destroy the device to determine cause of failure, possibly allowing the device to be used, depending on failure analysis results.

Gear drive assembly inspection was found to be of interest, particularly from the image quality obtained from the high-energy CT system. The 747 gear box ball bearing, bearing race, shims, and gear angles were adequately imaged. The CT results were highly encouraging to the Boeing manufacturing division and to the gear test group. However, there is no pressing need to move to CT as a routine inspection.

The penetration ability of high-energy CT on the hydraulic actuator was sufficient to image the entire 30 cm (12 in) length. A single CT slice in the longitudinal direction, if used during post-manufacturing inspection and if it contained suitable detail, would provide valuable assembly information such as O-ring position, mechanical arrangements, and clearances. The high-resolution data would be useful to organizations requiring analysis of such parts. There is nothing in the manufacture or repair of the units, however, that indicate a need for production engineering or inservice inspection in large quantities.

5.3 Recommendations

Based on the results of this study it recommended that additional effort be spent on investigating CT for thermal battery failure analysis and analysis of mechanical devices such as gear drives and actuators. This effort, however, should not be started until some time has been allowed for thoughtful review of the results obtained to date by interested parties. In particular, Boeing engineers are considering the closed systems results in several areas: 1) the thermal battery group is considering CT for special studies on high criticality and failed batteries, 2) the gear drive engineers are evaluating what information in the CT images can be useful for better product

development and 3) the failure analysis groups are considering the CT results from the actuator for possible follow-on applications. It is anticipated that interest will continue to grow in these three areas. Final testing plans will be defined when these interests show a clearly defined direction of study beyond the results of this report.

APPENDIX A

CT PHANTOMS

A set of CT phantoms was developed for the CTAD program in order to provide consistent evaluation of results from various CT systems. The phantoms serve several purposes. First, they provide a quantitative measure of the CT machine capability that can be used repetitively to assure consistent performance. Second, the quantitative measurements can be used in conjunction with part images to assess a quality level necessary to achieve desired detection or measurement levels in the inspected parts. Third, the phantoms can be used to select CT systems based on the desired sensitivity level for the CT application.

The use of phantoms for CT is complicated due to the wide range of parameters in any CT inspection. Therefore, caution must be used in extrapolating phantom data to suggest a "best" overall CT system. In fact, CT systems have varying designs that result in a range of performance characteristics. The phantoms allow the user a quantitative measure of quality level that, combined with other operating parameters, may suggest an optimum system. While the phantoms used in this program measure line pair resolution and contrast sensitivity, there are several other important parameters a user must be concerned with in selecting a machine for scanning: scan time, field of view, object penetration, data manipulation, system availability and cost.

Three basic phantoms types have been constructed. They are: line pair resolution phantom, contrast sensitivity phantom and a density standard phantom. The resolution and contrast sensitivity measurements are fundamental measures of a system. The density measurement is more of a calibration.

A1 Resolution Phantom

Figure A1-1 shows the line pair resolution phantom. The phantom consists of sets of metallic and acrylic plates of specified thicknesses. Line pairs of 0.5, 1, 2 and 4 lp/mm are formed by the phantom.

The entire assembly is bolted together and the line pair plates can be changed if additional or a different range of line pairs is desired. Following CT scanning the reconstructed image is analyzed by measuring the modulation of the CT numbers resulting from a trace across the line pairs. The modulation at each line pair set is measured as a percentage of the modulation, where the modulation measured between the 3 mm (0.12 in) thick metal and 3 mm (0.12 in) thick acrylic steps is 100 percent. Operating parameters such as field of view, slice thickness, integration time and detector collimation will affect the results. It is desirable to obtain data at CT machine parameters that are the same as that used for part scanning. The resolution phantom has been fabricated in two forms, steel/acrylic and aluminum/acrylic. The steel/acrylic phantom is for systems of 300 kVp and up, the aluminum/acrylic phantom is for systems under 300 kVp.

Figure A1-1 Photo of the resolution phantom

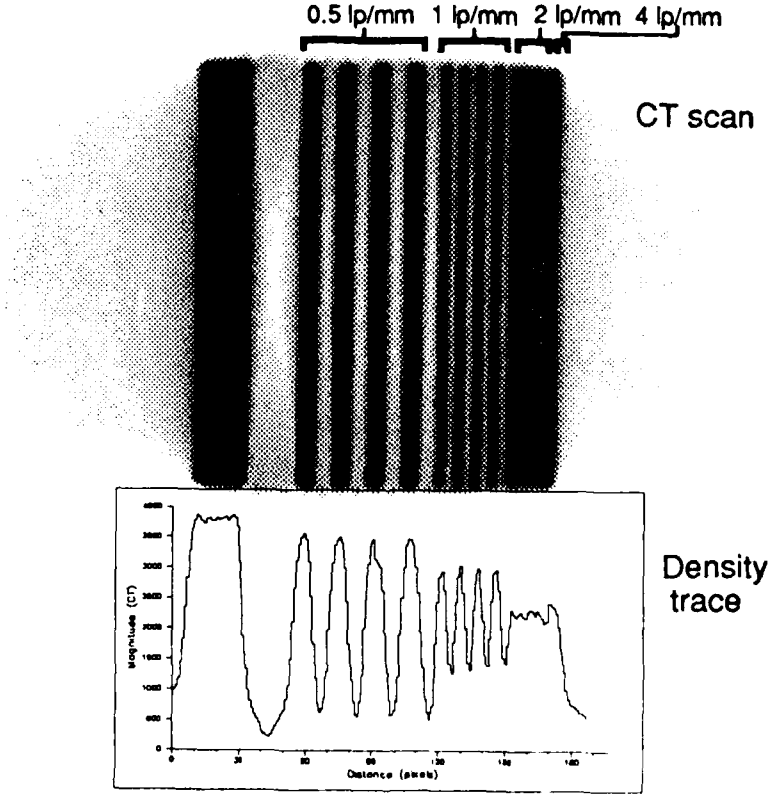

Figure A1-2 CT slice taken on the resolution phantom

high-resolution CT machine. The CT image density contour line across the gauge indicates modulation for the respective line pair measurements at approximately 82 percent at 1/2 lp/mm, 46 percent at 1 lp/mm, 4 percent at 2 lp/mm, and 0 percent at 4 lp/mm.

A2 Contrast Sensitivity Phantom

The contrast sensitivity phantom is a uniform disc of aluminum, 25 mm (1 inch) thick. Two sizes were made, one is 140 mm (5.5 inch) in diameter and the other is 70 mm (2.76 inch) in diameter. The smaller diameter size is used on systems with small fields of view or low kVp. Figure A2-1 shows an example CT slice of the large aluminum contrast sensitivity phantom with the corresponding density trace.

The measurement of contrast sensitivity is obtained by taking a region in the reconstructed image and determining the average and standard deviation for all CT numbers in the region. A typical region size of 1 cm (0.39 inch) diameter is used. Readings are usually taken at the center of the disk. The ratio of the average to the standard deviation is used as a signal to noise measurement. The inverse is a measure of contrast sensitivity. The signal to noise measurement for the density trace shown in Figure A2-1 is approximately 6.

The signal to noise ratio measurements are an important measure of system performance. The values improve with higher signal strengths. They also improve with smoothing algorithms in the reconstruction; however, this will decrease the resolution. Thus, the signal to noise and resolution must be considered together in assessing a quality level for performance.

A3 Density Calibration Phantom

The density calibration phantom construction drawing is shown in Figure A3-1. It consists of an acrylic disk of 140 mm (5.5 inch) diameter with inserts of ten various materials.

The CT numbers for each insert from the reconstructed image are plotted against the known densities to serve as a calibration curve for the machine. The insert materials vary in atomic number which adds another variable in the process when the X-ray energy is such that the photoelectric effects are significant. Nevertheless, the phantom is useful for indicating the general density sensitivity and accuracy of a CT machine. A CT scan of the density calibration phantom is shown in Figure A3-2.

The calibration plot for a 420 keV CT system is shown in Figure A3-3. The CT number (or density), averaged over a small region in the center of the insert, is plotted along the horizontal axis and material density along the vertical axis.

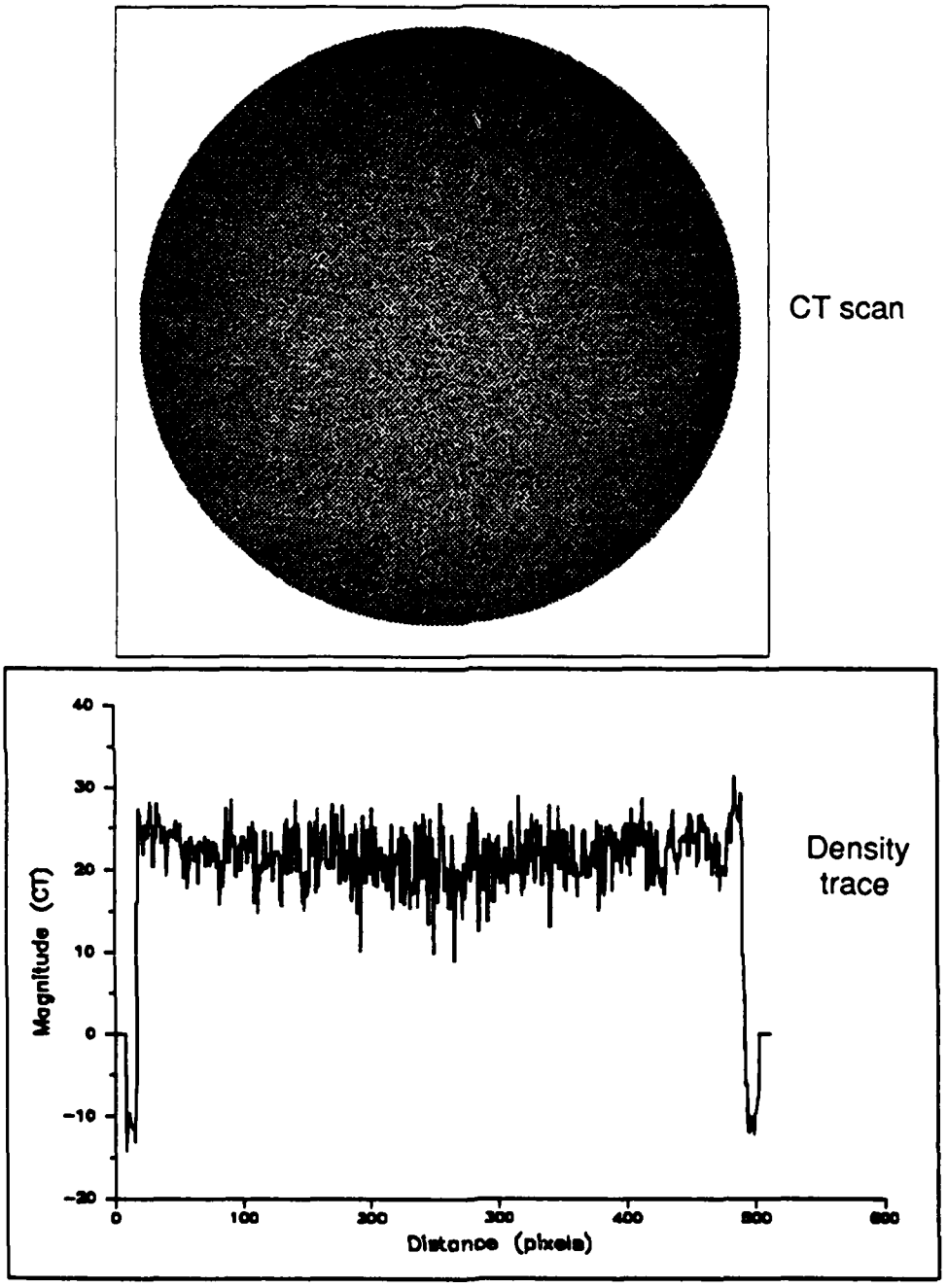

Figure A2-1 CT slice of contrast sensitivity standard

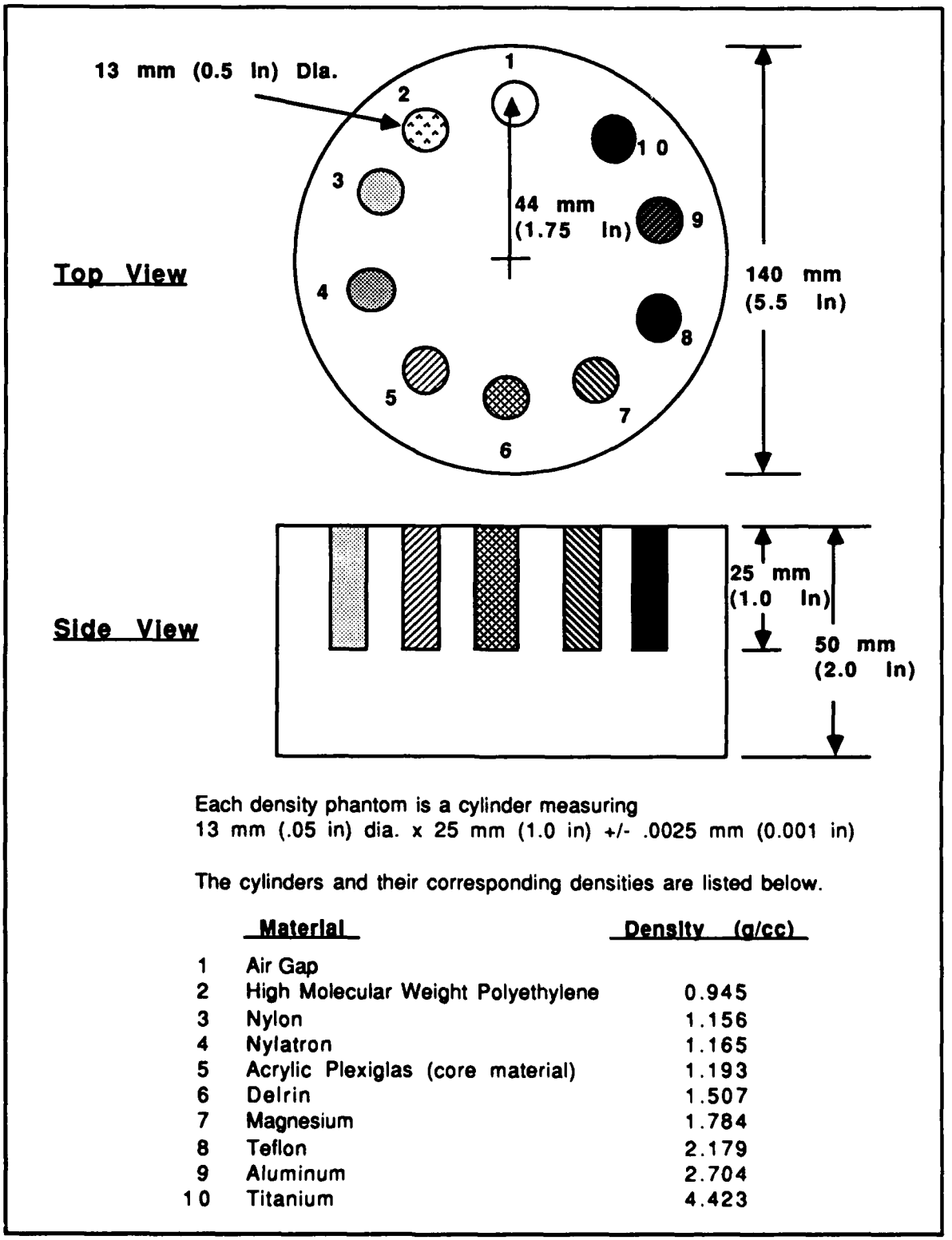

Each density phantom is a cylinder measuring
13 mm (.05 in) dia. x 25 mm (1.0 in) +/- .0025 mm (0.001 in)

The cylinders and their corresponding densities are listed below.

	Material	Density (g/cc)
1	Air Gap	
2	High Molecular Weight Polyethylene	0.945
3	Nylon	1.156
4	Nylatron	1.165
5	Acrylic Plexiglas (core material)	1.193
6	Delrin	1.507
7	Magnesium	1.784
8	Teflon	2.179
9	Aluminum	2.704
10	Titanium	4.423

Figure A3-1 Density calibration standard

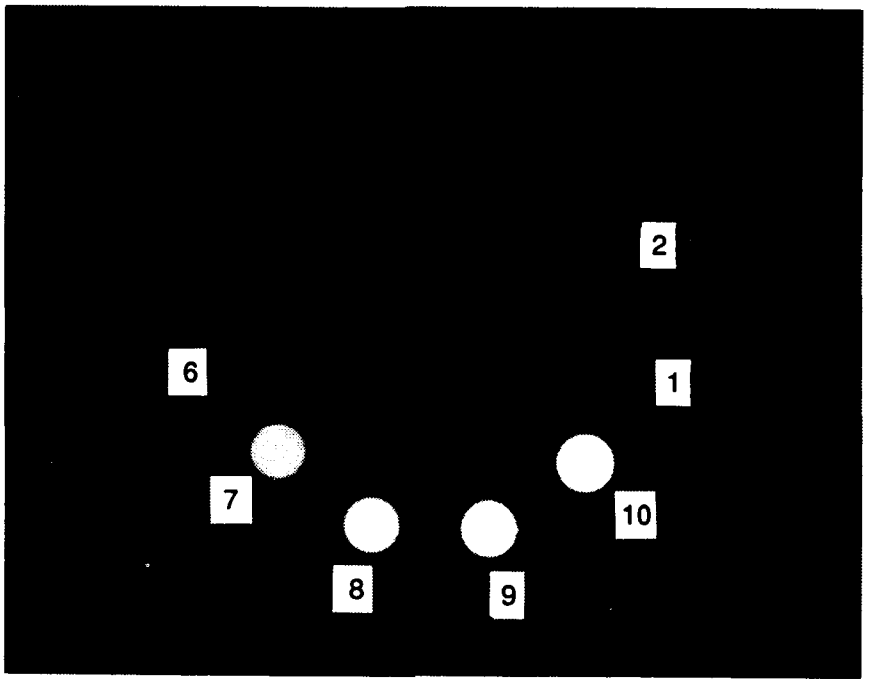

Figure A3-2 CT scan of density calibration phantom

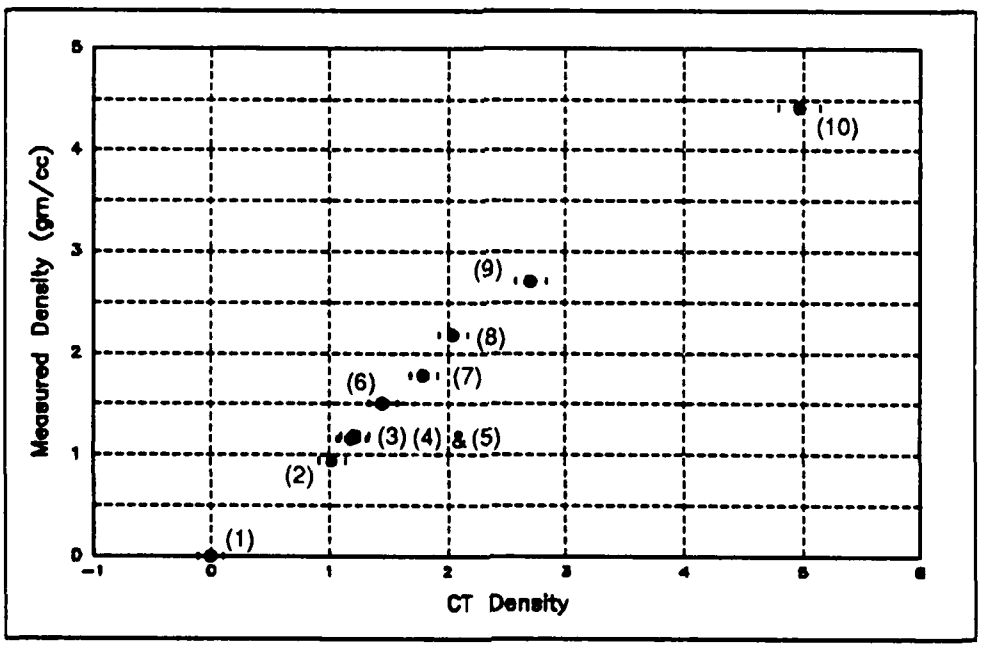

Figure A3-3 Calibration plot for density phantom

APPENDIX B

X-RAY IMAGING TECHNIQUES

The three techniques of X-ray imaging used in the closed system task assignment are film radiography, digital radiography, and computed tomography.

B1 Film Radiography

Conventional film radiography, as illustrated in Figure B1-1, uses a two-dimensional radiographic film to record the attenuation of the X-ray radiation passing through a three-dimensional object. This results in a shadowgraph containing the superposition of all of the object features in the image and often requires a skilled radiographer to interpret. Additionally the technique utilizes a diverging beam of radiation which distorts the object features at positions away from the central ray. This is a parallax problem in the image that occurs in both the horizontal and vertical directions.

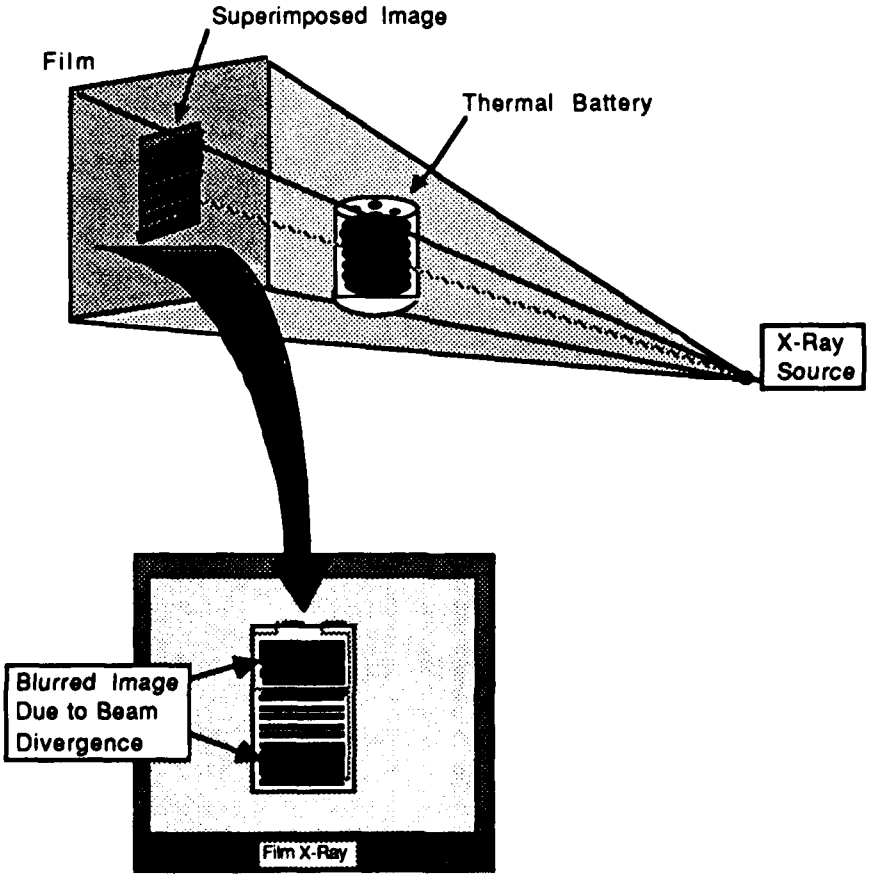

Figure B1-1 Shadowgraph image from film radiography

B2 Digital Radiography

Digital radiography (DR) is similar to conventional film radiography in that it is a shadowgraph image. The DR is performed on a system where the film is replaced by a linear array of detectors and the X-ray beam is collimated into a fan beam as shown in Figure B2-1.

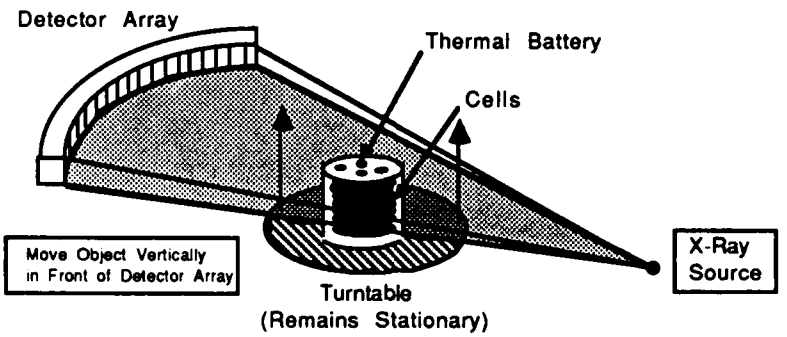

Figure B2-1 Digital radiography configuration

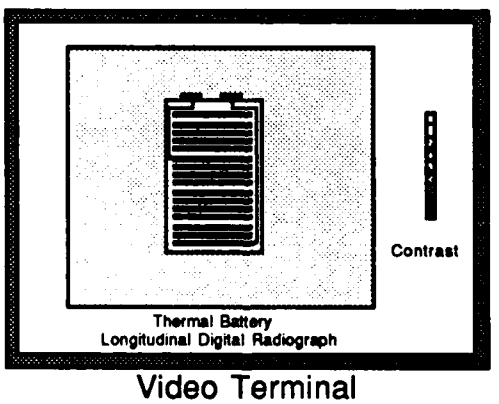

Figure B2-2 Longitudinal DR of thermal battery

The object is moved perpendicular to the detector array and the attenuated radiation is digitally sampled by the detectors. The data is 'stacked' up in a computer memory and displayed as an image as shown in Figure B2-2. Because the radiation is collimated in one direction but allowed to spread out in the other direction, parallax will occur only in the direction across the detector array.

B3 Computed Tomography

Computed tomography (CT) produces cross-sectional images of thin planes of an object. To generate a CT image, X-ray attenuation is sampled by an array of detectors using many viewing angles about the object (Figure B3-1). A computer mathematically reconstructs the cross-sectional image from the multiple-view data collected (Figure B3-2). A primary benefit of CT is that features are not superimposed in the image thus making it easier to interpret. Parallax is not a problem in CT imaging.

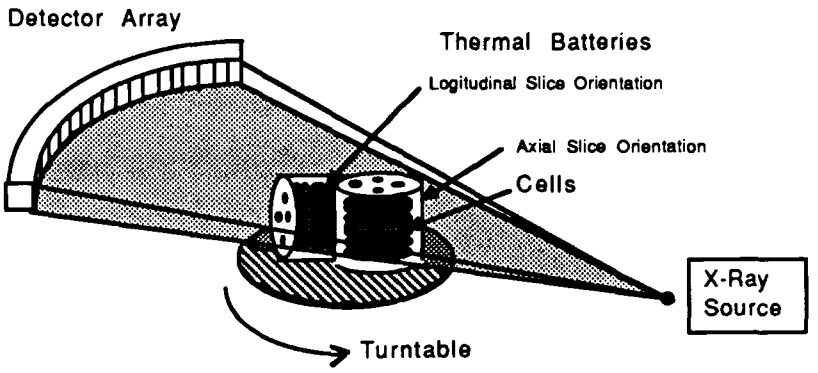

Figure B3-1 Computed tomography System features

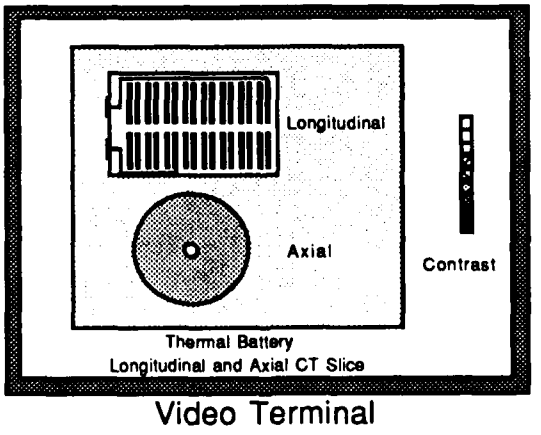

Figure B3-2: Computed tomography reconstruction

* U.S. GOVERNMENT PRINTING OFFICE: 1990 748-056/24109